PHYSIOLOGY

A long-term ketogenic diet causes hyperlipidemia, liver dysfunction, and glucose intolerance from impaired insulin secretion in mice

Molly R. Gallop[1,2], Renan F.L. Vieira[1,2], Peyton D. Mower[1,2], Elijah T. Matsuzaki[1,2], Willisa Liou[3], Faith E. Smart[1,2], Seth Roberts[1,2], Kimberley J. Evason[4,5], William L. Holland[1,2], Amandine Chaix[1,2]*

Ketogenic diets (KDs)—very-low-carbohydrate and very-high-fat diets—have gained popularity as therapeutic against obesity and type 2 diabetes. However, their long-term effects on metabolic health remain understudied. Here, we show that, in male and female mice, a KD protects against weight gain and induces weight loss but over time leads to the development of hyperlipidemia, hepatic steatosis, and severe glucose intolerance. Unlike mice on conventional high-fat diet, KD-fed mice remain insulin sensitive and display low-insulin levels. Hyperglycemic clamp and ex vivo glucose-stimulated insulin secretion assays revealed systemic and cell-intrinsic impairments in insulin secretion. Transcriptomic profiling of islets from KD-fed mice indicated endoplasmic reticulum (ER)/Golgi stress and disrupted ER-Golgi protein trafficking, which were confirmed by electron microscopy showing a dilated Golgi network consistent with defective insulin granule trafficking and secretion. Together, these results suggest that long-term KD leads to multiple aberrations of metabolic parameters that caution their systematic use as a health-promoting dietary intervention.

INTRODUCTION

A ketogenic diet (KD) is a very-high-fat, low-carbohydrate diet that has been used to manage refractory epilepsy for the past hundred years (*1*, *2*). The exact mechanisms by which a KD confers seizure control are unknown, but there are a few hypotheses including lowering and stabilizing blood glucose (BG), inducing favorable changes to brain metabolism, neurotransmitter levels and synaptic activity, and anticonvulsant effects of ketone bodies themselves (*3*–*5*). While a KD does not have a defined macronutrient content, as a treatment for epilepsy, it is generally first prescribed at a 4:1 ratio of 4 g of fat for every gram of carbohydrate or protein translating to ~90% of calories coming from fat (*2*, *6*). This high proportion of energy intake from fat causes the body to use fat rather than glucose as the primary fuel source and to enter a state of increased ketone body production, known as ketosis (*1*, *7*).

Ketone bodies are produced primarily in the liver when glucose and insulin levels are low such as during prolonged fasting or when consuming a ketogenic diet. In the 1960s, it was proposed that this state of low glucose and insulin, associated with the consumption of a KD, could treat obesity and related metabolic health conditions by favoring fat usage over fat storage (*7*). In addition, for similar insulin- and glucose-lowering reasons and potential benefits of ketone bodies themselves, a KD has been proposed to treat cancer and Alzheimer's disease, increase longevity, and improve metabolic health (*8*, *9*). However, a breadth of evidence to support these claims is lacking. A recent study found that a KD increases cellular markers of aging in mice (*10*), and in 2019, Journal of the American Medical Association (JAMA) released a publication titled "The Ketogenic Diet for Obesity and Diabetes—Enthusiasm Outpaces Evidence" (*11*). While a KD successfully control seizures in some people, its benefits will not necessarily translate to treating other diseases. In particular, pre-existing conditions—such as obesity, diabetes and hyperlipidemia—might interact with a KD in ways that have not been fully characterized in the predominantly young and limited group of epilepsy patients that have typically been studied (*6*, *12*). Therefore, harmful interactions between a KD and metabolic health conditions may negate the generally accepted belief that a KD is a clinically safe dietary intervention. From a nutritional and cardiometabolic standpoint, it is conceivable that there could be long-term ramifications to consuming a diet primarily composed of fat with very few carbohydrates that have been largely underexplored (*13*–*17*).

Previous studies in mice fed a KD have reported conflicting findings on metabolic health. For example, compared to mice on a chow diet, most studies observed a lower body weight (BW) on KD (*18*–*22*), but others saw weight gain (*9*, *23*, *24*). In contrast to the weight benefits found in many KD studies, high levels of blood cholesterol and nonesterified fatty acids (NEFAs) have been observed in multiple strains of mice on KD (*18*, *20*, *22*, *25*, *26*). Furthermore, the effects of a KD on glucose homeostasis have led to discordant and partial results. While some studies reported improvements in static BG without a glucose challenge (*21*, *25*, *27*) and improved glucose tolerance not only in wild type but also obese and diabetic models (ob, db, and stz) (*19*, *28*), others reported insulin resistance (*29*), glucose intolerance (*24*, *30*, *31*), and loss of β cells (*30*, *31*). A recent study reported diminished glucose-stimulated insulin secretion (GSIS) in 10 of the 13 inbred strains of mice (*32*). The inconsistencies in the macronutrient compositions of different KDs, together with differences in total caloric intake—since many studies use a calorie-restricted KD—and duration of the feeding protocol could potentially explain incongruencies between studies. Overall, possible cardiovascular risks associated with heightened lipid levels and inconclusive results on glucose homeostasis warrant further investigations into the long-term effect of KD consumption to define the conditions in which it can be helpful or harmful.

[1]Department of Nutrition and Integrative Physiology, University of Utah, Salt Lake City, UT, USA. [2]Utah Diabetes and Metabolism Research Center, Salt Lake City, UT, USA. [3]Electron Microscopy, Health Science Center Cores, The University of Utah, Salt Lake City, UT, USA. [4]Department of Pathology, University of Utah School of Medicine, Salt Lake City, UT, USA. [5]Huntsman Cancer Institute, University of Utah, Salt Lake City, UT, USA.
*Corresponding author. Email: amandine.chaix@utah.edu

Another important factor when considering the effects of KD resides in the study design, namely, whether a KD was used to prevent versus treat metabolic health conditions. In humans, KD is a very popular weight loss (WL) intervention, an effect that has been replicated in mice (*18*, *33*, *34*). However, WL per se may not be sufficient to normalize metabolic complications. For example, serum dyslipidemia and liver steatosis seem to persist despite reductions in weight under KD (*18*, *33*). Moreover, the effects of KD-induced WL on glucose regulation are also unclear: Some studies noted improvements in glucose tolerance testing (*18*, *33*, *34*), while some did not (*35*). Noticeably, hypoglycemia, a known complication of treating type 2 diabetes, was observed in mice on KD (*28*, *33*, *34*), which raises concerns about the safety of using KD in a population taking diabetes medication (*36*). Last, studies of KD-induced WL describe a reduction in high-fat diet (HFD)–linked hyperinsulinemia, yet we noted that in most, insulin levels dropped below that of chow-fed animals, which could be detrimental in the context of regulating fat storage and gluconeogenesis. Our search for preclinical studies characterizing KD-mediated WL only identified five studies thus far (*18*, *28*, *33*–*35*). With the mainstream popularity of KD as a therapeutic for obesity and diabetes, it is critical to further establish the broad metabolic effects of WL under KD, its effects on pre-existing metabolic conditions, and possible sex differences in these responses using a well-defined diet and a systematic metabolic characterization.

This study investigated the effects of long-term ad libitum feeding of a ketosis-causing KD on overall metabolic health in male and female C57BL/6J mice over the course of almost 1 year. The effects of a KD on BW and on multiple parameters of metabolic health were compared to those of a standard low-fat diet (LFD), a low-fat moderate protein (LFMP) diet with protein content matched to the KD, and the 60% HFD classically used in diet-induced obesity studies. The inclusion of both sexes allowed a direct analysis of sex differences in metabolic response to the different diets. Last, we also tested the metabolic effects of KD-induced weigh loss in obese males and females.

RESULTS

A 90% fat KD prevents weight gain as compared to an HFD in both male and female mice

Adult C57Bl/6J male and female mice were placed on one of four long-term diet regimens—a 10% fat LFD, a standard 60% HFD, an 89.9% fat KD, or another type of LFD with 10% fat and 10% protein to match the protein content of the ketogenic diet (LFMP) (Fig. 1, A and B). Male and female mice were maintained on the different feeding interventions for 36 and 44 weeks, respectively. To validate that this KD was ketogenic, blood levels of the most prevalent blood ketone body β-hydroxybutyrate (BHB) were measured, and the respiratory exchange ratio (RER) was also investigated. BHB levels were significantly elevated in the LFD, LFMP, and HFD groups in the fasted state as compared to the fed state (Fig. 1, C and D). However, in KD fed mice, the levels of BHB were elevated regardless of feeding:fasting status and were also significantly higher than any other group regardless of feeding status. We also monitored the RER in indirect calorimetry chambers to interrogate substrate usage in males on LFD, HFD, and KD. RER records shows that mice on LFD alternate between more carbohydrate burning during the feeding phase to more fat burning during the fasting state (fig. S1A). In contrast, HFD RER oscillations are severely dampened with an average value of 0.78. Mice on KD display a flat RER with even lower RER values of 0.73 suggestive of constant ketosis regardless of time-of-day or feeding status (fig. S1A). Together, these data suggest that the KD used in this study produces a constant state of ketosis.

Although the KD is 89.9% fat, male and female C57Bl/6J mice on KD were prevented from weight gain as compared to mice on a 60% HFD (Fig. 1, E and I). Both males and females on 60% HFD rapidly gained weight with BW divergence between the HFD and the LFDs observed as early as 1. BW gain on KD was slower and diverging from LFDs only after over 10 weeks in males (Fig. 1E) and 11 weeks in females (Fig. 1I). BW remained significantly lower in KD mice than HFD mice at all times (Fig. 1, E and I). At the end of 36 weeks, male mice on HFD weighed 54 g versus 43 g on KD (Fig. 1E). In female mice, after 44 weeks, mice on HFD weighed 60 g versus 35 g for mice on KD (Fig. 1I).

In males, weight gain on KD was mainly due to changes in fat mass as no changes in lean mass were observed across 26 weeks (Fig. 1, F and G). This is different to mice on HFD, in which weight gain was also predominantly due to increased fat mass, but changes in lean mass were also observed with mice on HFD gaining 19 g of fat mass and 8 g of lean mass after 26 weeks (Fig. 1F). Further, in HFD-fed males, fat mass accrual was maximal after 12 weeks and plateaued between weeks 12 and 26, but lean mass increased throughout the whole study (Fig. 1, F and G). In both males on HFD and KD, fat mass was higher than in the LFD group from week 4 at any time onward. However, lean mass was only greater in the HFD, and lean mass was not different between LFD and KD groups. After 26 weeks on the diets, although the mice on HFD had more fat and lean mass, the body fat percentage was not different between HFD- and KD-fed males (42.7 ± 1.6% fat for HFD 35.7 ± 5.1% fat for KD) (fig. S1B). In females, weight gain on a KD was due to increases in both lean and fat mass with mice gaining roughly 3.5 g of lean mass and 13 g of fat mass (Fig. 1, J and K). Similar to the males, females on HFD gained most of their weight through increase in fat mass but had a higher proportion of weight gain coming from fat with a ~29.5-g increase in fat mass and 7-g increase in lean mass (Fig. 1, J and K). After 27 weeks, females on HFD had 63.7 ± 1.2% body fat versus 46.7 ± 3.7% fat on KD (fig. S1).

The differences in weight between groups can at least partially be explained by differences in food intake (Fig. 1, H and L). Average food intake in male and female mice was highest in mice on HFD followed by mice on KD. This difference between HFD and KD was significant in male mice with mice on HFD consuming 13.4 kcal versus 11.1 kcals on KD and 8.4 kcals and 10.3 kcals for LFD and LFMP, respectively (Fig. 1H). Furthermore, throughout 36 weeks of food intake monitoring, the mice on HFD consumed more than the other groups, although this difference was more pronounced early on, it remained for the duration of the study (fig. S1D). Throughout the study, mice on KD also consumed an intermediate amount of calories that was higher than the LFD groups and lower than the HFD group (fig. S1D). In contrast to the males, female mice consumed less food overall with mice on HFD consuming 10.2 kcals versus 8.9 kcals on KD and 7.8 kcals and 7.6 kcals for LFD and LFMP, respectively. However, in female mice, the only significant difference in food intake was between the HFD and LFMP with HFD versus LFD having a marginally significant difference. This lack of significance between HFD and KD and HFD and LFD is likely because of the low cage number since food intake was measured as average cage intake each week (Fig. 1L). There were no differences in food intake between the LFD groups neither in males nor in females (Fig. 1, H

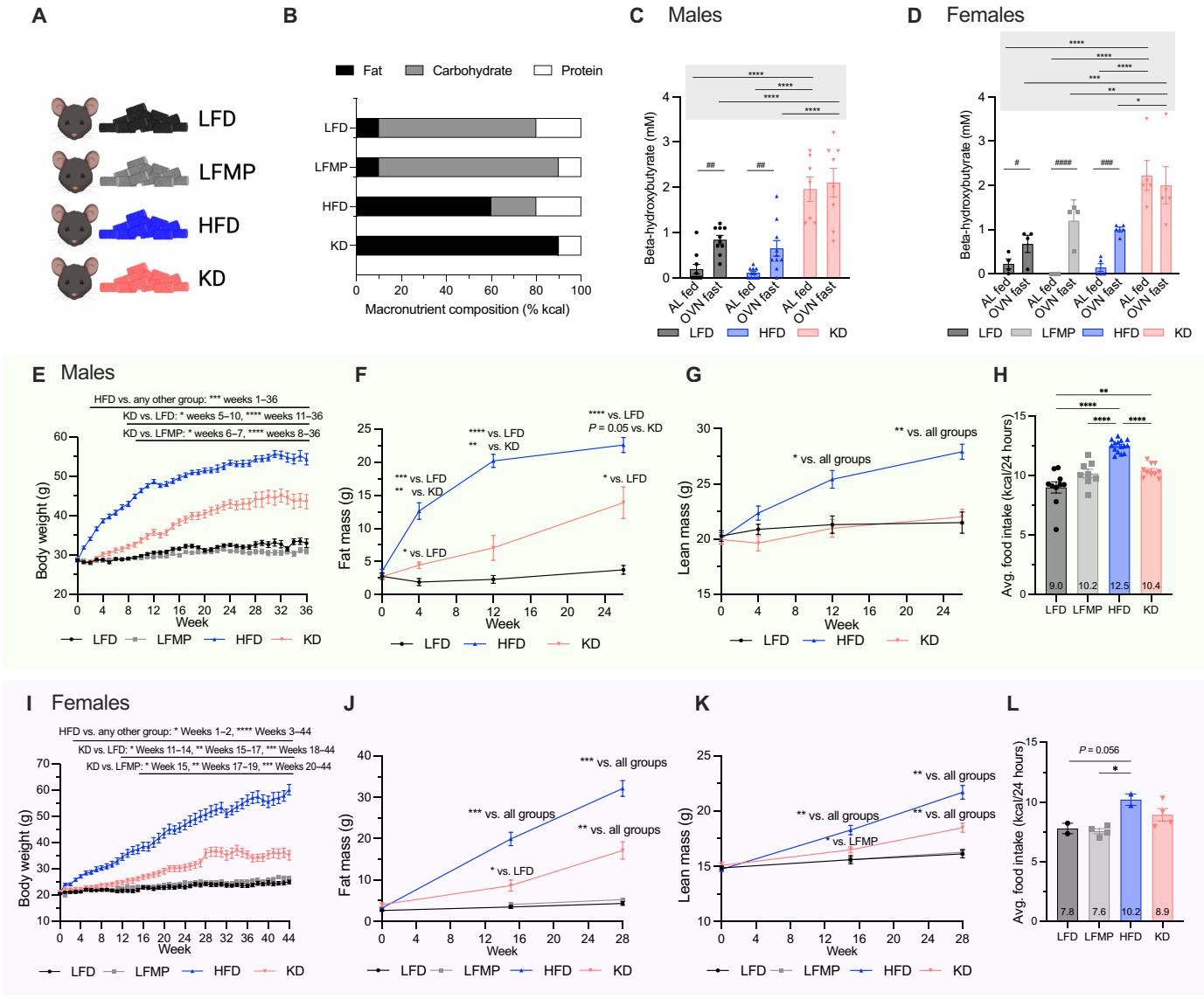

Fig. 1. Mice on KD are protected from weight gain as compared to mice on HFD. (**A**) Diets and color scheme used throughout the paper. (**B**) Macronutrient composition of diets used. (**C**) Male fed and fasted beta-hydroxybutyrate levels taken at 4 weeks [overnight (OVN) fast] and 6 weeks [ad libitum (AL) fed]; $n = 7$ to 10 per group. (**D**) Female fed and fasted beta-hydroxybutyrate at 15 weeks on diets ($n = 4$ to 5 per group). (**E**) Male BW pooled from three independent cohorts ($n = 30$ to 50 per group). (**F** and **G**) Male body composition ($n = 5$ to 6 per group): (F) fat mass and (G) lean mass. (**H**) Average 24-hour food intake from 36 weeks of data collection from three independent cohorts ($n = 8$ to 14 cages per group). (**I**) Female BW pooled from two independent cohorts ($n = 10$ to 20 per group). (**J** and **K**) Female body composition ($n = 5$ to 10 per group): (J) fat mass and (K) lean mass. (**L**) Average 24-hour food intake from 26 weeks of data collection from two independent cohorts over ($n = 2$ to 4 cages per group). Statistics: One-way ANOVA was used for (H) and (L), and mixed effects ANOVA was used for all other comparisons, post Hoc testing used Tukey's HSD test. *$P < 0.05$, **$P < 0.01$, ***$P < 0.001$, ****$P < 0.0001$; # only used for within group comparisons, #$P < 0.05$, ##$P < 0.01$, and ###$P < 0.0001$. Data are represented as means ± SEM.

and L). During the first week that the females were on the intervention diets, the HFD group consumed significantly more than the other groups, and while this difference declined, the HFD group still consumed more than other groups throughout the study (fig. S1D).

KD-fed mice have severe plasma hyperlipidemia and males have liver steatosis and dysfunction

Because ~90% of the calories in the KD are from fat, we assessed lipid homeostasis in KD-fed mice. In both males and females, plasma triglycerides (TGs) were significantly higher in KD-fed mice than in any other group including HFD-fed mice (Fig. 2, A and B). In general, TG levels were lower in females than in males, yet the TG increase on KD was similar in both sexes wherein TG levels were 1.7 times higher in KD than HFD fed mice (336 versus 193 in males and 152 versus 92 in females). Similar to the changes in TG, plasma NEFA levels were significantly higher in KD-fed mice versus other diet groups—2.75 and 1.8 times higher in KD versus HFD in males and females, respectively (Fig. 2, C and D). There were not sex differences in NEFA levels (Fig. 2, C and D). Plasma cholesterol (Cho) responses to the diets were different than that of TG and NEFA, with

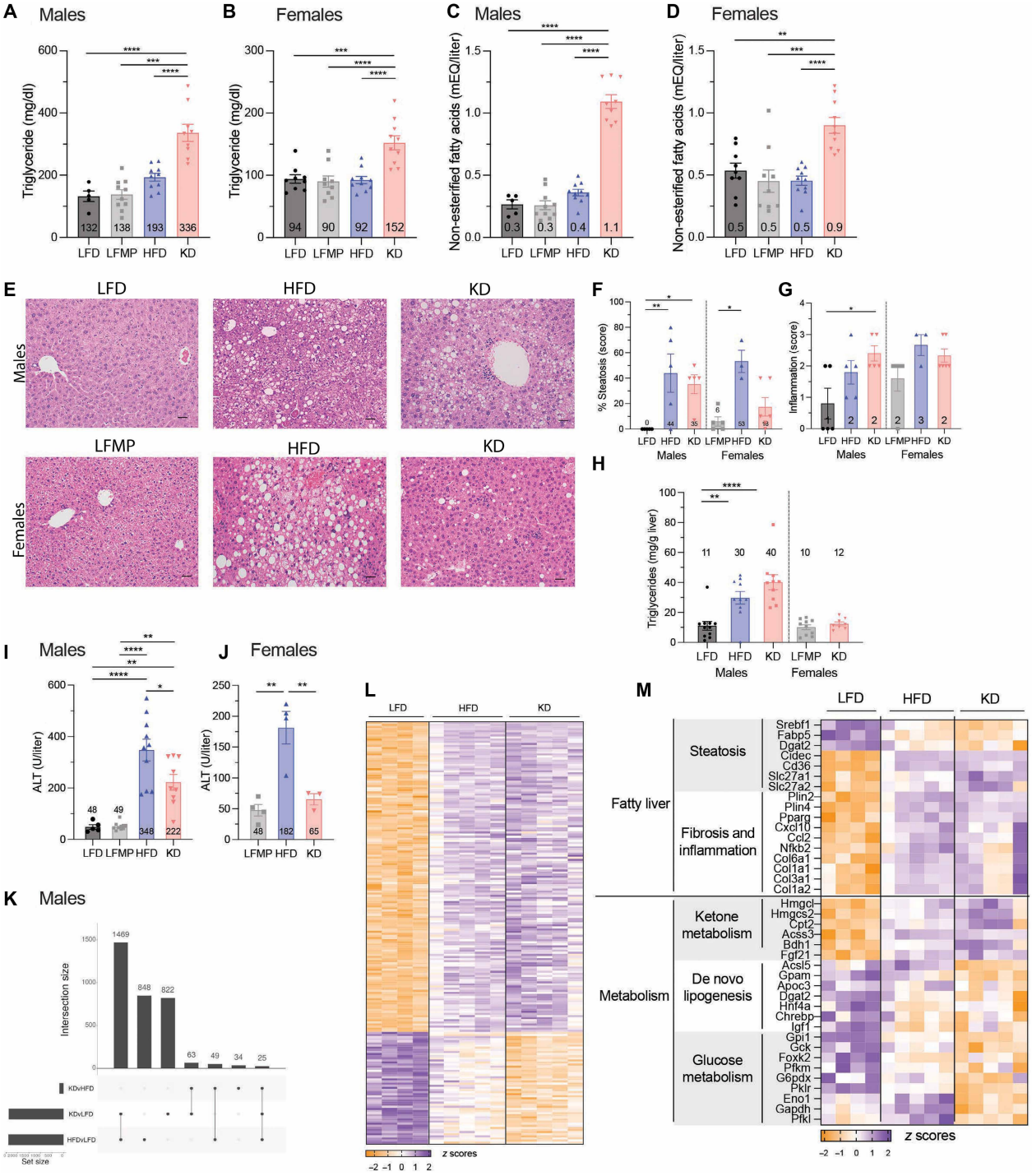

Fig. 2. A long-term KD causes dyslipidemia regardless of sex, and males have steatosis and liver dysfunction. (**A** and **B**) Plasma TG and (**C** and **D**) NEFAs in [(A) and (C)] males ($n = 5$ to 10 per group) and [(B) and (D)] females ($n = 9$ to 10 per group) after 32 and 15 weeks on diets, respectively. Blood samples were collected in the fed state. (**E**) Representative images from males (top) and females (bottom) on diet for 28 and 33 weeks, respectively. Scale bars, 20 μm. (**F** and **G**) Liver scoring by a pathologist blinded to conditions (male, $n = 5$ per group; female, $n = 3$ to 6 per group). (F) Steatosis as estimated percent visual field containing fat. (G) Inflammation score from 0 to 3 based on average number of inflammatory foci per visual field with five visual fields scored as described in (*90*). (**H**) Liver TG in males from two independent cohorts on diets for 28 and 38 weeks ($n = 10$ to 11 per group) and females ($n = 8$ to 10 per group) on diets for 33 weeks. (**I** and **J**) Plasma alanine aminotransferase (ALT) levels in males [(I), $n = 5$ to 10 per group] and females [(J), $n = 9$ to 10 per group] after 32 and 15 weeks on diets resp. (**K** to **M**) Liver bulk RNA sequencing (males, 38 weeks on diets, $n = 4$ to 5 per group. (K) UpSet plot comparing all DE genes. [(L) and (M)] Heatmap of (L) the top 200 most significant DE genes and (M) selected genes associated with steatosis, fibrosis, and metabolism between LFD and KD. Color intensity represents the z score based on $\log_2$ expression values. Statistics: [(A) to (F) and (H) to (J)] Data are represented as means ± SEM. One-way ANOVA with Tukey's post hoc testing with P values as: $^*P < 0.05$, $^{**}P < 0.01$, $^{***}P < 0.001$, and $^{****}P < 0.0001$. (G) Kruskal-Wallis test with Dunn's multiple comparison tests for post hoc analyses. [(K) to (M)] RNA sequencing statistics were determined using DESeq2 analysis with a Wald test and Benjamini-Hochberg correction. Significant genes had an adjusted P value of <0.05.

similar elevations in Cho levels in both HFD- and KD-fed mice as compared to mice on either of the LFDs (fig. S2, A and B). Together, we found, that in contrast to HFD, KD significantly raises plasma TG and NEFA levels in both male and female mice, suggesting an overabundance of fat is still present in the body, although mice on KD are leaner than mice on HFD.

The hyperlipidemic profile of KD-fed mice prompted us to assess liver health and function in male and female mice. Hematoxylin and eosin–stained (H&E) sections of livers collected after 6 months of dietary interventions were examined by a board-certified liver pathologist blinded to the feeding regimen. In males, steatosis, as estimated by the percentage of area made up of lipid droplets, was higher in mice on HFD and KD as compared to mice on LFD and was not different between HFD- and KD-fed mice (Fig. 2F). In females, only the livers from HFD mice had significant steatosis with no differences between LFMP- and KD-fed females (Fig. 2F). The visual inflammation scoring did not reveal marked or significant differences between any groups other than a possible trend to higher inflammation in both HFD- and KD-fed mice in both sexes (Fig. 2G). These results were confirmed using biochemical quantification of hepatic TG content (Fig. 2H). Male mice on long-term 6 to 9 months KD and HFD had significantly elevated liver TG content as compared to mice on LFD (three to four times higher), whereas female mice on KD did not have elevated liver TGs (Fig. 2H). Together, these results suggest that steatosis is similar between males and females on long-term HFD but only appears in males under KD, suggesting sex differences in the liver response to KD. Last, we measured plasma alanine transaminase (ALT) as a readout of liver function. In males, after 32 weeks of their respective diets, HFD- and KD-fed mice had roughly 7 and 4.5 times higher ALT compared to LFDs, respectively (Fig. 2I). In addition, ALT was significantly lower in KD versus HFD males. In females, after 48 weeks on their respective diets, mice on HFD and KD also had elevated ALT. ALT was not different between mice on LFD and KD, but the HFD group had ALT levels that were 3.8 and 2.8 times the levels of mice on LFMP or KD, respectively (Fig. 2J). Overall, these findings indicate liver dysfunction and steatosis under KD feeding in males but not females, suggesting that there are sex differences in the liver response to KD.

To evaluate how HFD versus KD affected hepatic lipid handling at the molecular level, we compared the liver transcriptome of KD-, HFD-, and LFD-fed males. Gene expression profiles were very similar between mice on HFD and KD, with only 171 differentially expressed (DE) genes (adjusted $P < 0.05$) between mice on KD and HFD compared to 2351 for HFD versus LFD and 2371 for KD versus LFD (Fig. 2K). The gene expression profiles of the top 200 DE genes between KD and LFD were virtually identical for HFD and KD (Fig. 2L), and many of these genes are associated with steatosis, fibrosis, and inflammation in agreement with our histology and biochemical findings (Fig. 2M). Thus, at the gene expression level, while both HFD and KD livers are different from mice on LFD, the livers from mice on HFD and KD are almost indistinguishable. Because of the constant state of ketosis observed in KD mice, we specifically interrogated the expression of genes involved in ketogenesis and glucose metabolism. Genes linked to ketone body metabolism—such as 3-hydroxy-3-methylglutaryl-CoA synthase 2 (*Hmgcs2*), which controls the rate limiting state in ketogenesis, and β-hydroxybutyrate dehydrogenase 1 (*Bdh1*)—were as expected increased under KD, yet, interestingly, similar expression patterns were also observed in HFD (Fig. 2M). In addition, genes involved in de novo lipogenesis such as *Chrebp* and *Dgat2* were down-regulated in both HFD and KD livers as compared to LFD (Fig. 2M). Expectedly, genes related to glycolysis and glucose metabolism were lower in KD as compared to either HFD or LFD (Fig. 2M). Overall, liver histological, biochemical, and molecular analysis revealed that, although mice on a KD are leaner than mice on an HFD, the males still suffer steatosis and inflammation that likely impair their liver function.

Mice on KD have severe glucose intolerance and impaired insulin secretion

We next examined how KD affects glucose homeostasis compared to a traditional 60% HFD and LFDs. In the first 4 weeks of the intervention, mice on KD had lower fasting BG levels compared to HFD and lower postprandial glucose compared to both HFD and LFD (Fig. 3A). However, when tested after a longer time, between 27 and 32 weeks for males and 15 weeks for females, fasting glucose was similarly elevated in HFD- and KD-fed mice compared to LFDs (Fig. 3, B and C). Fed BG remained significantly lower in KD-fed versus HFD-fed males and females and LFD males likely due to the very low amount of carbohydrates in the diet (Fig. 3B). These results suggest that while a KD may be beneficial for regulating (hyper)glycemia in the short term, long term KD feeding is associated with fasting hyperglycemia, similar to that observed under HFD, and fed hypoglycemia. We next assessed the ability of the mice to restore glycemia after an intraperitoneal bolus of glucose. Intraperitoneal glucose tolerance test (GTT) revealed glucose intolerance similar to HFD-fed mice after 11 weeks in males and 31 weeks in females (Fig. 3, D and G). However, much more severe glucose intolerance was observed in males after 33 weeks on the diet: KD males reached a maximum glucose of 539 mg/dl versus 427 mg/dl in HFD, and BG only decreased by 95 mg/dl versus 168 mg/dl in HFD after 2 hours despite KD mice receiving less glucose based on their lower BW (Fig. 3E). In females, we also observed a deterioration of glucose response over time on KD with glucose intolerance being more severe after 31 weeks than 15 weeks (Fig. 3, F and G).

To assess how quickly glucose dysregulation develops on a KD, we performed longitudinal GTT assessments in males. We found that glucose intolerance was present as early as 1 week on KD (fig. S3D), and this glucose intolerance became more severe over time (fig. S3, D to F). Severe glucose intolerance was not limited to intraperitoneal injections as it was also observed upon oral administration of glucose (oGTTs) and upon oral mixed meal tolerance tests in mice on KD (fig. S3, A to C). Together, these findings show that male and female mice on long-term KD develop glucose intolerance that worsens over time.

To test whether glucose intolerance in KD-fed mice was due to insulin resistance, we performed insulin tolerance tests (ITTs). After 11 weeks on the diet interventions in males, fasted BG was similar between HFD and KD groups and significantly higher than LFD groups (Fig. 3H). Upon insulin injection, BG dropped markedly within the 15 min with a delta or slope that was not different between KD and the LFDs groups (−118.2 mg/dl in LFD, −97.7 mg/dl in LFMP, and −114.0 mg/dl in KD) but significantly less in HFD (−63.2 mg/dl in HFD) (Fig. 3, H and I). A similar response was observed in females at 29 weeks (Fig. 3, L and M). When an ITT was performed in males after at 32 weeks on their respective diets, the response to insulin was maintained in KD and LFD mice while the HFD-fed males hardly responded (Fig. 3, J and K). Together, these results confirmed the well-characterized insulin resistance of males

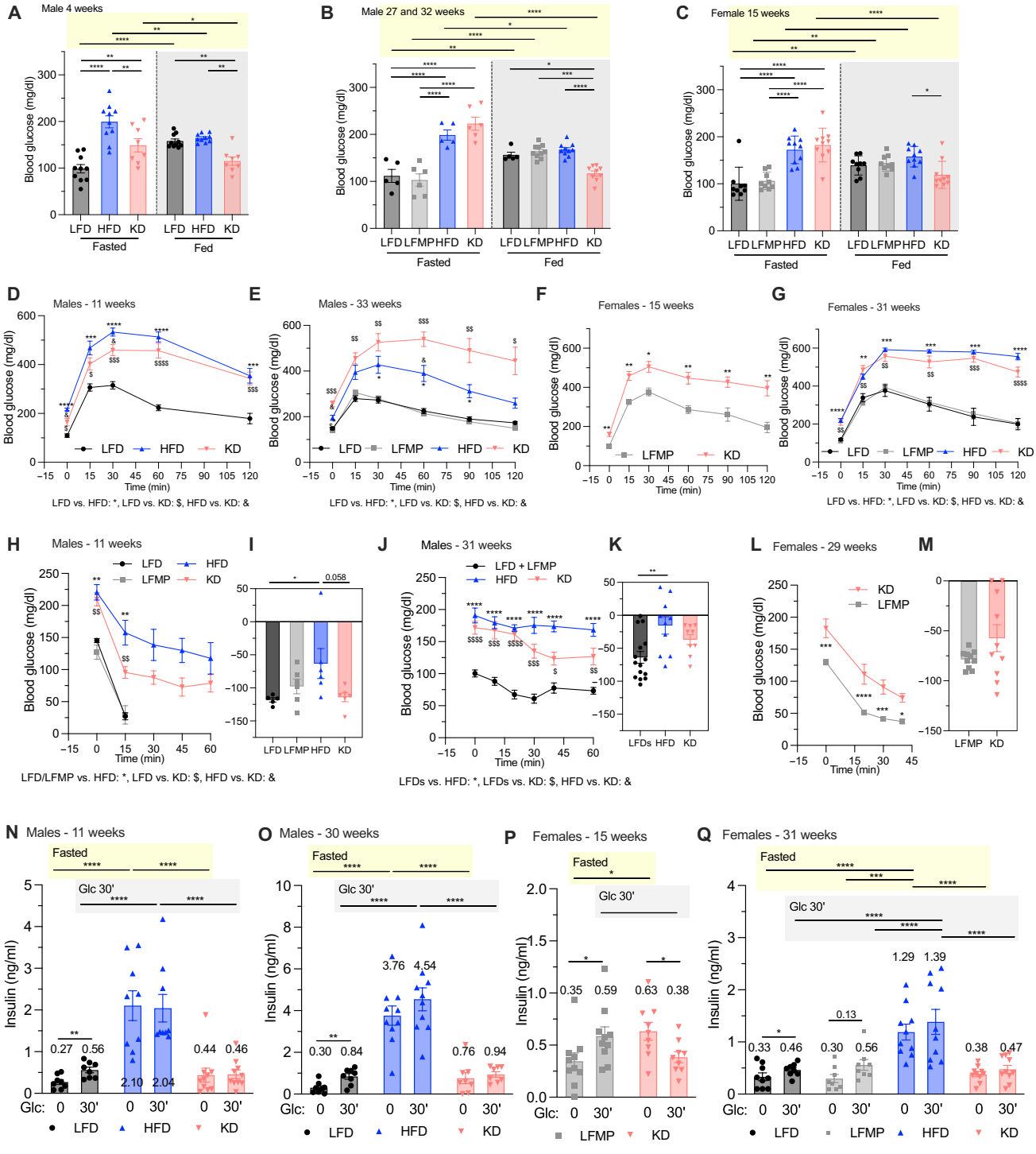

Fig. 3. A long-term KD causes severe glucose intolerance and suppresses insulin secretion. (**A** to **C**) Fasted and fed BG. Fasted glucose was measured at 7 a.m. (onset of dark cycle) following a 14-hour fast, and fed glucose was measured at 11 a.m. during the dark cycle. (A) Males after 4 weeks ($n = 8$ to 10 per group), (B) 27 and 32 weeks on diet from two independent cohorts ($n = 5$ to 10 per group). (C) Females after 15 weeks on diets ($n = 4$ to 9 per group). (**D** to **G**) Glucose tolerance tests (GTTs) with a bolus of glucose (1.5 mg/g) given after an overnight fast (over the light phase) in: (D) males after 11 weeks on diets ($n = 8$ to 10 per group), (E) males after 33 weeks on diets ($n = 5$ to 6 per group), (F) females after 15 weeks on diets ($n = 9$ to 10 per group), (G) females after 31 weeks on diets ($n = 8$ to 10 per group). (**H** to **M**) Insulin tolerance tests with insulin (0.75 U/kg). Bar graphs [(I), (K), and (M)] show the slopes in the first 15 min (I) or 30 min [(K) and (M)]. [(H) and (I)] Males after 11 weeks on diets ($n = 5$ per group). [(J) and (K)] Males on diets for 31 weeks ($n = 5$ to 10 per group). [(L) and (M)] Females on diets for 29 weeks ($n = 5$ to 10 per group). (**N** to **Q**) Plasma insulin levels at baseline and 30 min after a bolus of glucose. Data in (N), (P), and (Q) are from the blood collected during the GTT presented in (D), (F), and (G), respectively. Data shown in (O) are from a separate experiment after 30 weeks on diets ($n = 8$ to 10 per group). Statistics: One-way or two-way ANOVA with Tukey's HSD for post hoc testing was used. Paired *t* tests were used to compare insulin levels between 0 and 30 min within a group. The number of symbols represents *P* values as: $*P < 0.05$, $**P < 0.01$, $***P < 0.001$, and $****P < 0.0001$. Data are represented as means ± SEM.

fed HFD. On the contrary, the significant drop in BG upon insulin injection showed that KD-fed male and female mice remained insulin sensitive and do not develop insulin resistant as HFD-fed mice do.

To determine whether glucose intolerance in KD-fed mice was instead due to a defect in insulin secretion, we measured plasma insulin levels in response to a glucose bolus using an in vivo GSIS assay. We found that, in males and females on LFDs and KD, baseline-fasted insulin levels were low and not different, in contrast to the HFD groups that had high insulin both prior and 30′ after the glucose injection, as would be expected with insulin resistance (Fig. 3, N to Q). LFD- and LFMP-fed male and female mice had a significant increase in insulin upon glucose injection at all longitudinal time points (Fig. 3, N to Q, and fig. S3, G to I; 0′ versus 30′ within diet comparisons). Despite being numerically modest, such an increase was sufficient to restore normoglycemia in about 1 houqr (see GTTs Fig. 3, D, F, and G, which are from the same experiments as the respective panels in Fig. 3, N, P, and Q).

Longitudinal assessment of GSIS over time spent on KD further revealed that the insulin secretion deficit in response to glucose occurred after 4 to 8 weeks of KD (fig. S3, G to I) and from at least 15 weeks onward in females (Fig. 3, P and Q), suggesting that a KD impairs islets function over prolonged feeding. The lack of glucose-evoked changes in insulin levels are consistent with the lack of BG regulation seen in the GTTs and corresponds to the further impairment of glucose tolerance over time.

Together, these results suggest that altered glucose homeostatic response in HFD-fed versus KD-fed mice is not caused by the same mechanism. While impaired glucose regulation in HFD-fed mice is likely linked to insulin resistance in the context of high insulin levels, impaired insulin secretion likely underlies glucose intolerance in KD-fed mice.

KD-fed mice have normal islets size and insulin content

The severe glucose intolerance and lack of glucose-evoked insulin secretion in the context a normal ITT in KD mice prompted us to examine the pancreas. We hypothesized that reduced islets number and/or insulin content may be involved in the lack of GSIS.

Because insulin secretion was impaired in mice on KD, we assessed differences in pancreatic islet size or number by histologic analysis. Since insulin secreting β cells make up the majority of cells in murine islets, we used insulin-/proinsulin-stained area to demarcate islets by immunochemistry. The average islet area was much larger in HFD- than KD- or LFD-fed mice, but there was no difference in size in KD compared to LFD islets (Fig. 4, A and D), while the number of islets per section was similar in all three groups (Fig. 4C). When examining islets size distribution by group, we found that mice on HFD had significantly fewer small islets and at least twice as many larger islets compared to the other groups (Fig. 4B and fig. S4B). We also found that the percent insulin positive area was not different between LFD and KD but was higher in the HFD group (fig. S4A). Mirroring the findings in males, there were no differences in average size, size distribution, or number of islets between females fed a KD or a LFMP (Fig. 4, E to G). Islet size and number were also comparable between males and females. To complement these histological findings, we quantified pancreas mass and insulin content. Pancreas mass was significantly increased in both HFD-fed males and females (Fig. 4, H and J) but was similar between mice on LFD and KD (Fig. 4, H and J). In agreement with our histological findings, HFD pancreas had more insulin per milligram tissue in both male and female mice (Fig. 4, I and K), while male mice in general had more insulin than female mice. The differences in pancreas size and insulin content also translated to the HFD having more total insulin per pancreas as compared to the KD and LFD mice (fig. S4, C and D). Overall, these results confirm the established effect of HFD feeding leading to islet hyperplasia and show that, unexpectedly, KD feeding was not associated with overt loss in islet mass or insulin content that could underly insulin secretion deficiency. Thus, because mice on KD can both produce and respond to insulin, we proceeded to test whether a defect in secretion could explain their glucose intolerance.

Mice on KD lose rapid insulin secretion in vivo and isolated islets have impaired insulin secretion

To delve further into the underlying cause of glucose intolerance in KD-fed mice, we performed an in vivo hyperglycemic clamp experiment in awake, freely moving mice. Throughout the 120-min clamp protocol, 50% glucose was infused through a jugular vein catheter to obtain 30 min of clamped BG at around 250 mg/dl for 30 min. To that end, BG was measured at regular intervals throughout, and the infusion rate titrated accordingly. Upon initial infusion, BG rapidly increased in all groups and peaked at 30 min (Fig. 5A). The glucose infusion rate (GIR) was then progressively lowered to bring the BG to the target 250 mg/dl, and the GIR was later increased after about 60 min to maintain the clamped target; a BG of 250 mg/dl was obtained in LFD- and HFD-fed mice between 90 and 120 min of the test (Fig. 5C). However, in KD-fed males, BG remained significantly elevated for 90 min despite the GIR being reduced to the minimum infusion rate possible from 50 min onward (Fig. 5C). BG in KD mice only started to decrease toward the end of the experiment (Fig. 5A). From 90 to 120 min, BG was effectively clamped at an average of ~230 mg/dl in HFD- and LFD-fed mice, but BG in KD-fed mice was significantly higher at 314 mg/dl and could not decrease to the target level during the course of the experiment (Fig. 5B) even in the context of significantly lower GIR (Fig. 5D). In parallel, we measured plasma insulin levels throughout the study (Fig. 5E). Upon glucose infusion, insulin levels significantly and rapidly rose in LFD and HFD (87 and 68% increase respectively), reaching max level at 15 min (Fig. 5, E and F). Strikingly, insulin levels in KD-fed mice initially decreased from 0 to 10 min; a slow rise in insulin levels was not apparent until 30 min post–glucose infusion (GI) start, and insulin levels peaked at 90 min that coincide with the time at which BG begins to decline (Fig. 5A). Insulin levels overall were higher in HFD than LFD during the clamp (Fig. 5E), which is indicative of insulin resistance. Because mice on KD have similar insulin levels to the control mice both at baseline and at the peak, this suggests that their glucose intolerance is caused by impaired insulin secretion rather than insulin resistance.

To assess cell-autonomous differences in insulin secretion, islets from males fed LFD, HFD, and KD for 60 weeks were isolated and tested by dynamic ex vivo GSIS using a perifusion system (Vanderbilt islet and pancreas analysis core). Baseline insulin secretion at 5.6 mM glucose (roughly equal to 100 mg/dl) was similar across all three groups. However, upon stimulation with 16.7 mM glucose (roughly 300 mg/dl), both KD and HFD islets secreted less insulin than LFD islets (Fig. 5G). Specifically, the initial peak in insulin secretion at 18 min was lower in both HFD and KD islets versus LFD islets (LFD: 4.7 ng/100 Insulin EQuivalent (IEG)/min versus HFD: 0.99 ng/100 IEQ/min KD: 1.9 ng/100 IEQ/min), and insulin levels remained

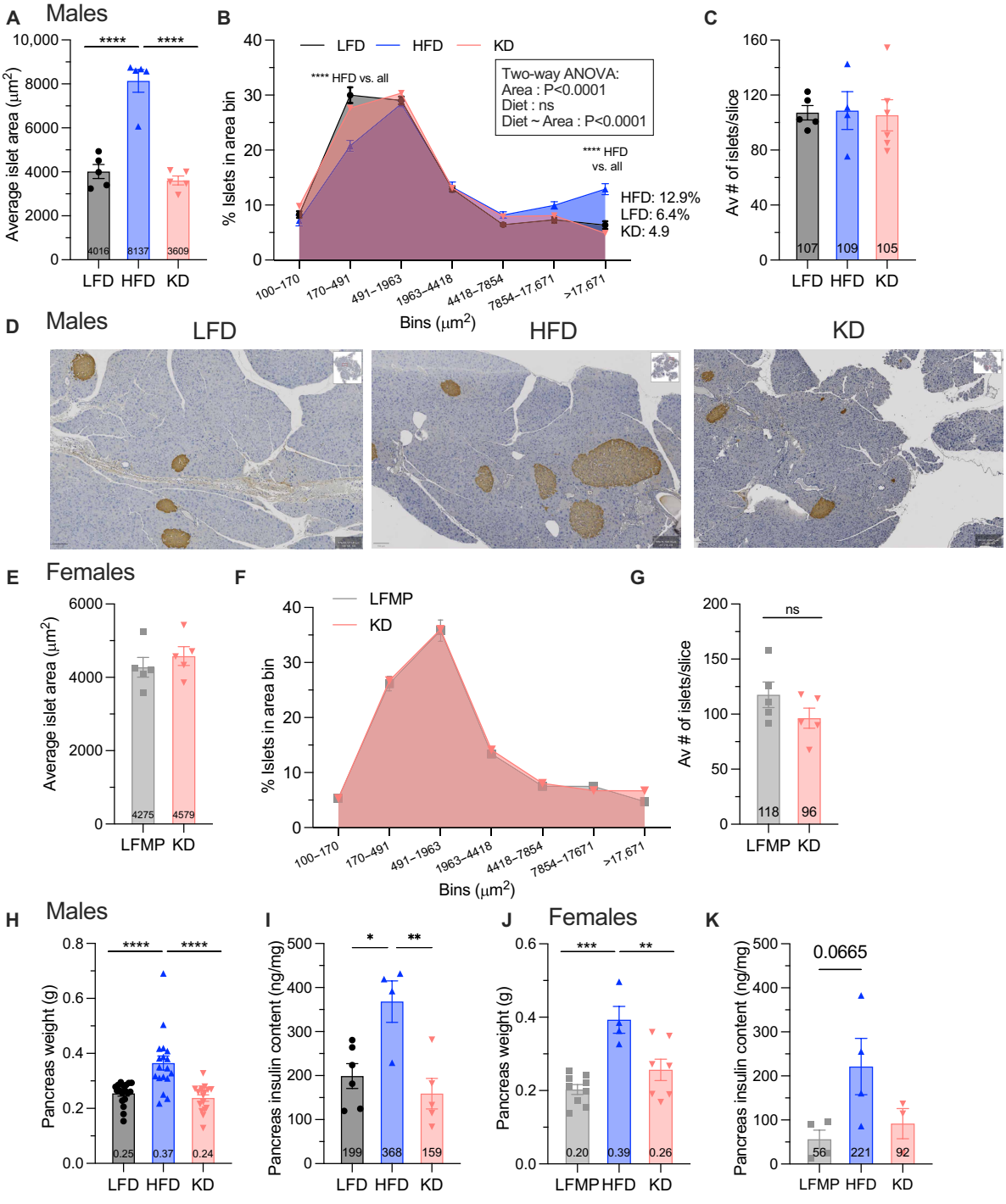

Fig. 4. A HFD but not a KD increases islet size, pancreas weight, and insulin content in the pancreas. (**A** to **G**) Analysis of chromogenic insulin/proinsulin staining in the pancreas with hematoxylin counterstain. Qupath was used to quantify islet area based on detection of the brown insulin stain. [(A) to (C)] Males, 8 to 12 slices were taken throughout the pancreas from $n = 4$ to 6 animals per groups for a total 5157 islets analyzed on LFD, 6718 on HFD, and 6389 on KD. [(E) to (G)] Females, six to seven slices were taken throughout the pancreas ($n = 5$ per group), for a total of 3749 LFMP and 3428 KD islets analyzed. [(A) and (E)] Average islet area. [(B) and (F)] Frequency distribution of islet sizes as number of islets per slice in each bin. Bins correspond to islet diameter 100 µm² = diameter of 11.3 µm or the size one β cell (and the minimum size needed to identify a nucleus and clear borders in the analysis); 170 µm² = diameter of 14.7 µm; 490.87 µm² = diameter of 25 µm; 1963 µm² = diameter of 50 µm; 4417.86 µm² = diameter of 75 µm; 7853.981 µm² = diameter of 100 µm; and 17,671 µm² = diameter of 150 µm. [(C) and (G)] Average number of islets per slice. (D) Representative images from male islets. Scale bar, 100 µm. (**H**) Male pancreas weight after 6 to 9 months on respective diets ($n = 17$ to 18 per group pooled from three independent cohorts) and (**I**) insulin content after 6 months on the diets ($n = 5$ to 6 per group). (**J**) Female pancreas weight ($n = 4$ to 8 per group) and (**K**) insulin content after 6 months on respective diets ($n = 3$ to 4 per group. Statistics: One-way or two-way ANOVA with Tukey's HSD for post hoc testing was used. The number of symbols represents P values as: *$P < 0.05$, **$P < 0.01$, ***$P < 0.001$, and ****$P < 0.0001$. Data are represented as means ± SEM.

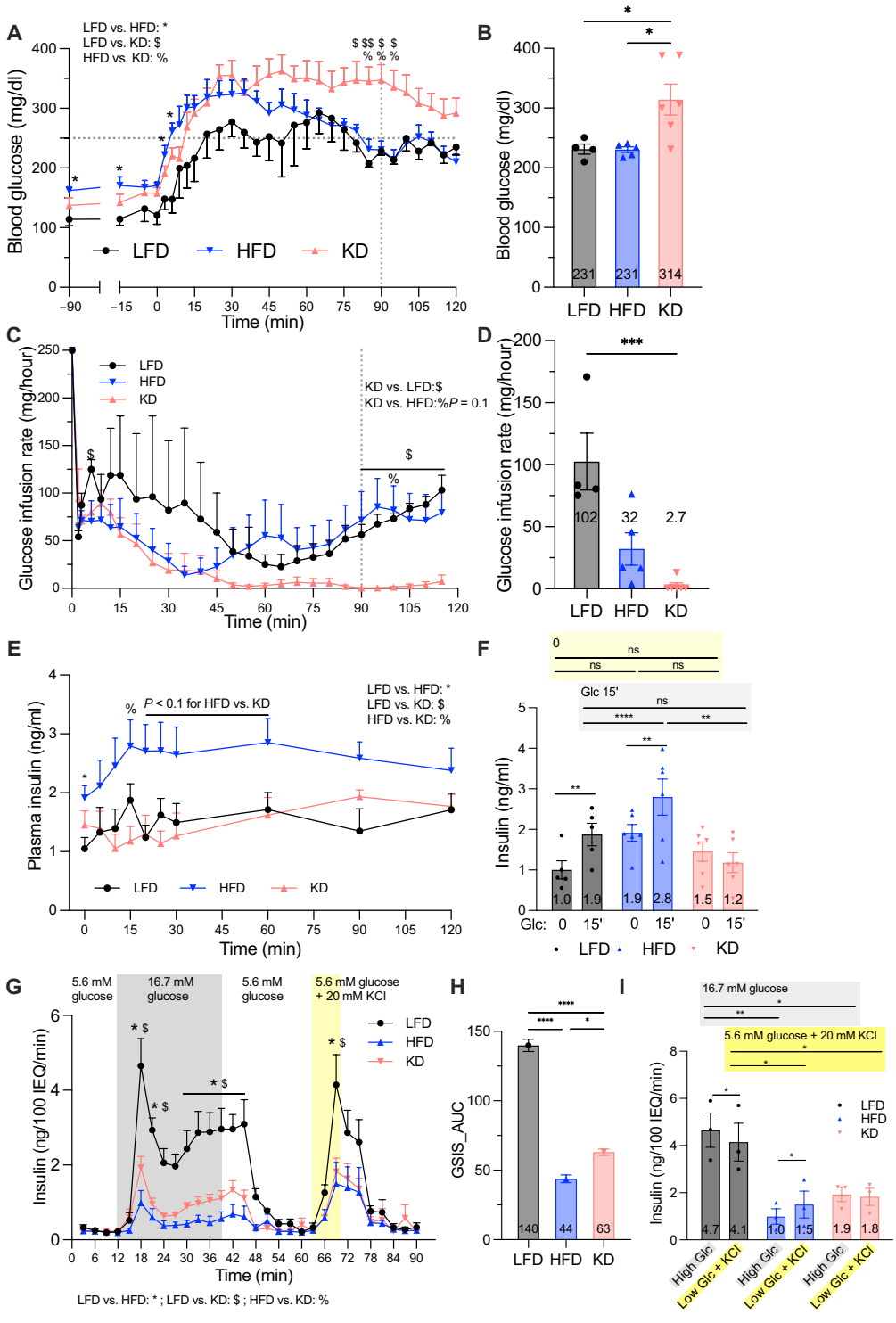

Fig. 5. Mice on KD lose rapid insulin secretion. (**A** to **F**) Measures taken during hyperglycemic clamp after 25 weeks on the respective diets. $n = 4$ to 6 male mice per group. Time courses of BG (A), the GIR (C), and plasma insulin levels (E) obtained via tail vein sampling. Average BG (B) and average GIR (D) during the 90 to 120 min when BG was clamped. (F) Insulin levels before and 15 min into the glucose infusion. (**G** to **I**) Ex vivo GSIS ($n = 3$ per group). (G) Insulin level over time during the different phase of the perifusion assay, wherein insulin level is normalized to 100 insulin equivalents (IEQ; 1 IEQ represents an islet with a diameter of 150 μm). (H) Total insulin secretion during the GSIS as calculated by the area under the curve (AUC) from (G). (I) Peak insulin secretion during high glucose and KCl stimulation [insulin levels from (G) at 18 and 69 min, respectively]. Statistics: One-way ANOVA (B, D, and H) or two-way ANOVA [(A), (C), (E), (G), and (I)] with post hoc testing using Tukey's HSD except in (H), which used Dunnett's multiple comparison test to compare HFD and KD with the LFD group only. The number of symbols above data denote the following P values: *$P < 0.05$, **$P < 0.01$, ***$P < 0.001$, and ****$P < 0.0001$. Data are represented as means ± SEM.

lower for KD and HFD throughout the high-glucose stimulation (Fig. 5G area marked by gray background). To determine whether this deficiency in insulin secretion is a result of improper glucose sensing versus dysfunctional insulin secretion, in the final step of the GSIS, islets were exposed to 20 mM potassium chloride (KCl), which depolarizes β cell in the absence of high glucose, thus allowing us to assess maximal insulin secretory capacity independent of glucose sensing. Under KCl, the HFD and KD islets secreted significantly less insulin than the LFD islets (Fig. 5, G and I). However, to determine whether this reduced insulin secretion under KCl is a result of glucose sensing versus aberrant insulin secretion, we must compare peak insulin secretion under glucose versus peak insulin secretion under KCl. For HFD islets, peak insulin secretion under KCl was higher than under 16.7 mM glucose (1.5 versus 0.99 ng/100 IEQ/min) (Fig. 5, G and I), suggesting a deficiency in glucose sensing in addition to aberrant insulin secretion. Conversely, for the KD islets, the peak insulin secretion under KCl and high glucose were similar (1.82 and 1.9 ng/100 IEQ/min), suggesting a deficiency in insulin secretion machinery but no problem with glucose sensing. Together, the results of dynamic GSIS testing suggest that insulin secretion is compromised in both HFD and KD compared to LFD yet possibly through different mechanisms. These results show that impaired insulin secretion in KD is linked to a secretory defect but not a glucose sensing defect as was the case in the HFD islets.

Transcriptomic and EM analysis of KD islets reveals ER-Golgi stress and aberrant Golgi function

Our findings thus far have established that the pancreases from KD-fed mice have impaired insulin secretion as compared to those from LFD/ LFMP and HFD fed mice. To gain insight into the molecular causes behind the secretory dysfunction in KD islets versus HFD islets, we analyzed the bulk transcriptome of isolated islets harvested from male mice fed LFD, HFD, or KD for 36 weeks. We found the most gene expression changes when comparing islets from mice on KD versus those from mice on LFD with a total of 1666 DE genes. Of those 1666 genes, 1083 were uniquely changed between KD and LFD, 397 distinguish KD versus both HFD and LFD, 175 changed in both KD and HFD compared to LFD, and a very small 11 genes were different between all dietary condition (Fig. 6A). In contrast, there were only 242 DE genes in HFD versus LFD (Fig. 6A), indicating that the KD altered the islet transcriptional profile much more than an HFD when compared to LFD. Last, comparing KD to HFD, there was a total of 1127 DE genes. Among those, 697 were changed only under KD versus HFD, whereas 397 changed in both KD compared to HFD and LFD, and a small 22 DE genes changed between KD versus HFD and HFD versus LFD) (Fig. 6A). Overall, transcriptomics analysis revealed 408 (397 + 11) DE genes that distinguish the islets from KD-fed mice from islets of mice fed either HFD or LFD—that is expression of these 408 genes were significantly different in KD versus both LFD and HFD conditions (Fig. 6A).

To identify potential mechanisms behind the KD-specific islet secretory dysfunction, we performed pathway enrichment analysis in Metascape using this list of roughly 400 genes that differentiate KD islets from HFD and LFD islets. Pathways linked to translation and peptide metabolism, ER stress, and ER to Golgi transport were specifically enriched in KD versus both LFD and HFD islets (Fig. 6B). In addition, the most significantly up-regulated gene in KD as compared to both HFD and LFD was *Creb3l3* (fig. S5, A and B), a member of the CREB3 transcription factor family that is activated by ER and Golgi stress (*37*). Because these analyses pointed at a potential ER and Golgi stress signature, we therefore performed a targeted analysis of genes related to "Golgi apparatus" [Gene Ontology (GO):0005794] and "response to endoplasmic reticulum stress" (GO:0034976) (Fig. 6C). Genes (158 of 1280; 12.3%) linked to Golgi and almost 20% (41 of 224) of GO-annotated ER stress genes showed significantly altered expression in KD islets versus LFD or HFD islets (Fig. 6C). This targeted analysis further evidenced severe ER-Golgi stress in the KD islets. Zooming out, we used the bigger list of KD versus LFD 1666 DE genes and Reactome to pathway analysis. Reactome identified significantly up-regulated pathways in KD linked to (i) translation (orange, 10 pathways), (ii) metabolism (blue, 4 pathways), (iii) Golgi-ER transport and coat protein complex II (COPII)-mediated vesicle transport (green, pathways), (iv) protein localization (dark green, 2 pathways), and (v) amino acid metabolism (yellow, 3 pathways). The similar enrichment of genes related to vesicle transport, ER/Golgi stress, and translation was also observed when KD and HFD islets were compared (fig. S5C). A color-coded schematic (Fig. 6E) shows that these altered pathways can influence insulin secretory capacity throughout the process of insulin synthesis and granules secretion. Targeted investigation/further probing the expression of genes involved into genes that are specifically involved in vesicle transport between the ER and Golgi and to the plasma membrane (as identified by Reactome and literature search) shows that many of these genes are significantly different between KD and both HFD and LFD (Fig. 6F). Together, the gene expression analysis suggests a unique dysfunction of the ER-Golgi transit in KD islets, which may underlie the KD-specific deficit in insulin secretion as both other groups secreted insulin in response to glucose during the clamp studies. Because up-regulation in protein trafficking mainly occurs pre-Golgi, we hypothesized that an impairment in Golgi processing causes an overall disruption in the production of mature insulin granules and, thus, looked specifically at genes involved in Golgi organization and transport. *Rab8b*, which was down-regulated in KD islets as compared to LFD and HFD islets, plays a role in transporting proteins from the Golgi to the plasma membrane, suggesting reduced protein export from the Golgi (*38*). In further support of impaired Golgi functioning is our observed down-regulation of *Rab30* and *Rab39*, which are necessary for Golgi apparatus organization (*38*, *39*). Last, we compared the 175 genes that were DE in KD versus LFD and HFD versus LFD, to identify a "high-fat" transcriptomic signature. We found that HFD and KD had reduced expression of genes related to immune function (fig. S5D), suggesting that the "high-fat" signature is immune related and does not alter vesicle transport or ER/Golgi stress.

To establish the relevance of these transcriptional findings, we obtained electron microscopy images of islets from LFD and KD islets. Islets, which represent less than 1% of the surface area of the pancreas, were identified at low magnification through a flower-like structures centered around a capillary (fig. S6A). B cells were identifiable by the presence of insulin granules, and some of them with characteristics insulin crystals (fig. S6A). Insulin granules were present in β cells from both KD and LFD islets. We interrogated marked visual differences in the pool of readily releasable insulin granules at the basal membrane that could explain the lack of rapid release of insulin in KD-fed mice. However, with these granules only making up about 1% of all insulin granules and not having any known defining features (*40*, *41*), we could not determine whether there were differences between LFD and KD (fig. S6A). However, when zooming

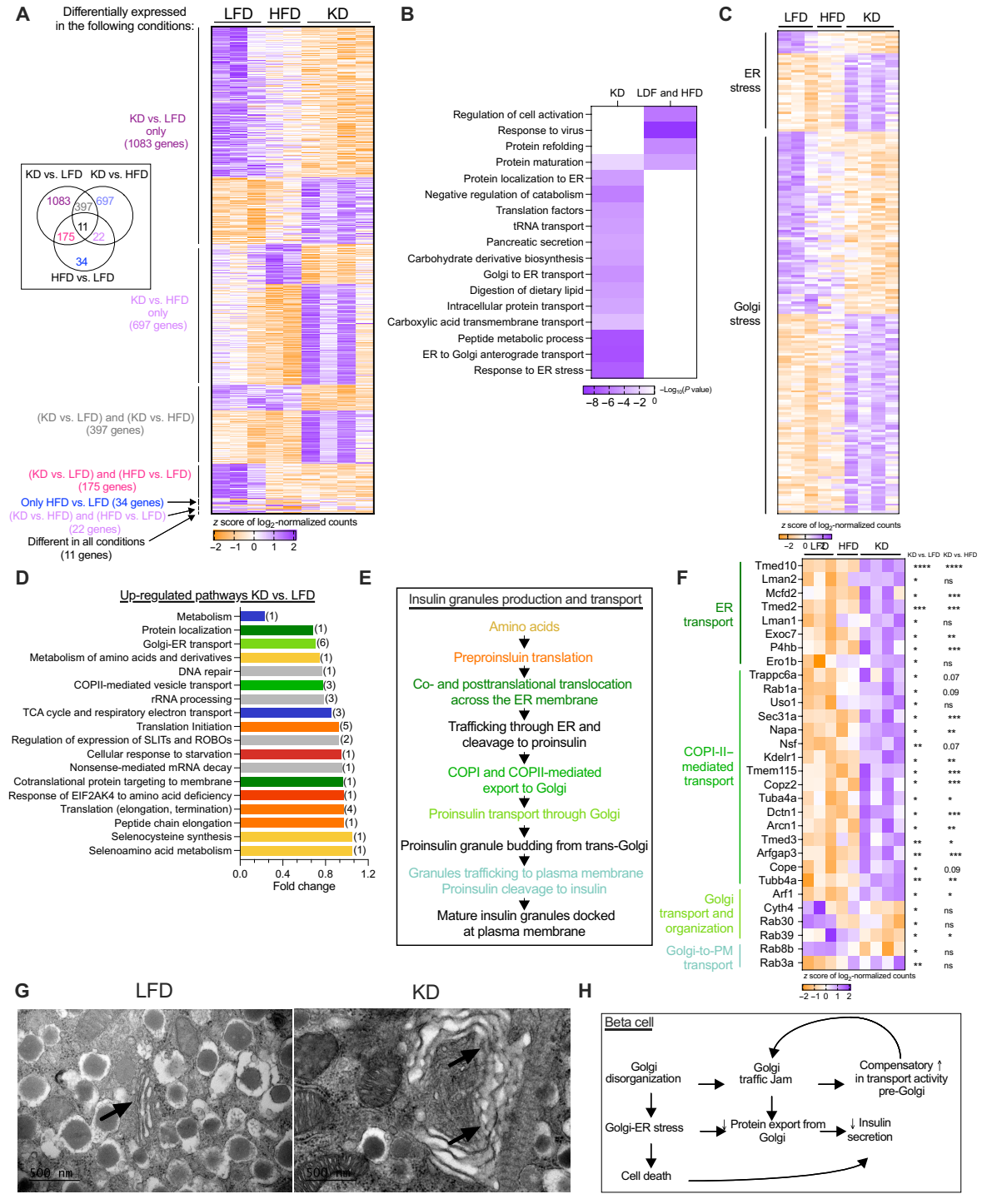

Fig. 6. Islet transcriptomic analysis reveals that KD causes ER Golgi stress and impaired protein transport. Bulk RNA sequencing from islets isolated from male mice after 36 weeks on interventions. (**A**, **C**, and **F**) Heatmaps showing *z* scores of $\log_2$-normalized expression. (A) Heatmap of all DE genes. The Venn diagram inset shows number of genes per comparison, and the colors correspond to the colored labels on the heatmap. (**B**) The 397 genes that were DE in both KD versus LFD and KD versus HFD were run through Metascape, which identified ontology categories that were enriched in one group versus the other as displayed in the heatmap; the purple indicates increased expression in the corresponding group, and the color intensity represents $-\log_{10}(P$ value) of the enrichment as calculated by Metascape. (C) Using the Gene Ontology database, we identified genes involved in ER and Golgi stress genes and plotted the genes that were significantly different in KD versus LFD. Heatmap of selected genes associated with ER-Golgi stress. (**D**) Significantly up-regulated pathways identified using Reactome Pathway analysis of DE genes between KD and LFD. False discovery rate < 0.05 for all pathways. (**E**) Pathway of insulin granule generation and processing. Colors in (E) correspond to colors in (D) and (F). (F) Heatmap of selected genes involved in protein processing and vesicular transport. (**G**) Electron micrograph images of pancreatic β cells showing Golgi dilation in KD. (**H**) Mechanism linking transcriptomic findings with reduced insulin secretion. Statistics: DE genes were identified using DESeq2 analysis with a Wald test and Benjamini-Hochberg correction. Significant genes had an adjusted *P* value of < 0.05.

on the ER-Golgi, the Golgi apparatus in KD β cells looked vastly different than in LFD, appearing dilated and vesiculating (Fig. 6G and fig. S6B). This dilation, swelling, and fragmentation of the Golgi would be consistent with deficient insulin secretion observed under KD feeding.

Together, we propose that a KD causes Golgi disorganization that impairs protein transport leading to compensatory up-regulation of trafficking in the ER and ERGIC and a down-regulation of proteins transported out of the Golgi in addition to significant ER-Golgi stress with both the stress and impaired protein trafficking suppressing insulin secretion and production (Fig. 6H).

While a KD induces WL, insulin secretion becomes severely impaired.

A KD is currently being used to treat obesity, diabetes, and metabolic syndrome despite few preclinical studies establishing its efficacy and effects on overall metabolic health. Our observation that over time, KD feeding impairs insulin secretion prompted us to evaluate insulin regulation in obese mice fed a 60% HFD subjected to KD-induced WL. Male and female mice rendered obese by 14 or 15 weeks of 60% HFD feeding, respectively, were then switched to a LFD (LFD or LFMP) or a KD. Noticeably, after 15 weeks of HFD, males had reached their maximal BW, whereas females weight continued to increase throughout the study (37.0 g at week 15 and 55.5 g at week 32; Fig. 7D). In males, while a KD induced immediate WL (Fig. 7A), the mice on KD lost much less weight than the mice switched to LFMP and even began to gain some weight back after week 20. After 9 weeks of WL, the mice on LFMP had lost almost four times as much weight as the mice on KD (LFMP lost 20.9 g and KD lost 5.4 g) (Fig. 7A). Females switched to the LFD and KD rapidly and markedly lost weight for the first 3 weeks after starting on the new diets and then gained a small amount of weight back, although their weight still remained far below that of mice on HFD in (Fig. 7D). Similar to the males, the females on LFD lost much more weight than those on KD, with females on KD ending up with a higher weight than before starting the KD (LFD lost 9.7 g, and KD gained 0.6 g). Overall, in both males and females, KD induced WL, but the LFDs were a more effective WL intervention than the KD. In both males and females, the early WL was accompanied by an initial drastic drop in food intake when switching from HFD to either KD or LFD/ LFMP (fig. S7, E and I). While food intake increased in mice on KD and LFD/LFMP, the intake remained lower than that of mice that remained on HFD showing that reduced food intake can at least partially explain reductions in weight (fig. S7, E, F, I, and J).

Because a KD caused high lipid levels in our prevention study, we also measured Cho and TG levels to determine whether KD-induced WL caused favorable changes in plasma lipids. We found that, while WL under LFD and LFMP was associated with lower Cho and TG levels, mice that lost weight under KD remained hyperlipidemic (fig. S7, G, H, K, and L). These findings suggest that while a KD can induce WL, it generally cannot reverse metabolic dysfunction.

Once BW had begun to stabilize—7 and 14 weeks into the WL interventions in males and females respectively—in vivo GTT and GSIS were performed. In both males and females, although the groups switched to KD had lost weight, the mice were as glucose intolerant as mice on HFD who had not lost any weight (Fig. 7, B and E). The measurement of blood insulin levels revealed that mice switched to LFMP and LFD no longer had hyperinsulinemia and had normal GSIS and glucose tolerance response (Fig. 7, B, C, E, and F). In contrast, while the males and females on KD now also had low insulin levels, insulin secretion in response to glucose was gone (Fig. 7, C and F). These results show that regardless of sex and regardless of BW at initiation of the WL intervention, KD induces WL but impaired insulin secretion occurs and prevents the normalization of glucose homeostasis.

We next wondered whether a KD could prevent or limit weight regain (WRG) following a WL intervention. To test this, a subset of mice that had gone through WL on KD or LFD/ LFMP were switched back to HFD (Fig. 7, A and D; WRG). Both male and female mice regained some or all of the lost weight after switching back to HFD, showing that a KD cannot prevent or cure diet induced obesity (Fig. 7, A and D). We also assessed whether a KD could cure HFD induced insulin resistance and performed in vivo GTT and GSIS at either 4 weeks after switching back to an HFD in males (Fig. 7, G and H) or 10 weeks after in females (Fig. 7, I and J). In males and females, following WRG, there was no protection against glucose intolerance or hyperinsulinemia (Fig. 7, G to J). In males and females, any reductions in insulin levels that accompanied WL with a KD or LFD were reversed following resumption of an HFD (Fig. 7, C, F, H, and J). Thus, while a KD causes WL, it does not cure the ensuing diabetes nor does it prevent WRG.

Because we observed severe islet dysfunction on a KD, we tested whether the effects of a KD on glucose tolerance were reversible. To our surprise, we found that, in male mice, 4 weeks after switching from a long-term KD to LFMP, the glucose intolerance phenotype disappeared (Fig. 7L), suggesting that at least some of the detrimental metabolic effects of KD are reversible. In summary, these findings show that while a KD causes WL following diet induced obesity, it cannot cure or permanently ablate glucose intolerance or impaired insulin secretion. Although the effects of KD are reversible, these experiments show that a LFD more favorably affects glucose tolerance, insulin secretion, and WL.

Last, to begin to understand whether the glucose and weight effects were a result of the specific macronutrient composition of our KD or could be generalized to other low-carbohydrate diets, we also included a group of mice on a high-fat high-protein diet (HFHP) for which the composition of fat matched that of the 60% HFD and the composition of carbohydrate matched that of our KD at 0.1% carbohydrates (fig. S7, M to P). The mice on the HFHP had similar BW, glucose tolerance, and insulin secretion to the mice on KD (fig. S7, M to O). While the HFHP group was phenotypically similar to the KD group, this group had significantly lower levels of KBs (KD: 2.0 mM versus HFHP: 0.4 mM), suggesting that the impaired insulin secretion we observed on KD would likely be observed in other low-carbohydrate HFDs as well.

DISCUSSION

The ketogenic diet has grown in popularity over the past several decades as a tool for improving weight and metabolic health. While a KD benefits in treating epilepsy are concrete, its effects on metabolic health have been largely understudied. In particular, changes in glucose metabolism upon KD are not fully understood. As most people who go on a KD will likely consume glucose eventually due to the difficulty to strictly adhere to a KD long term (*3*), this is of critical importance for patients using a KD to treat obesity and related metabolic conditions such as type 2 diabetes. In addition, the very high-fat content of the diet can challenge whole body regulation

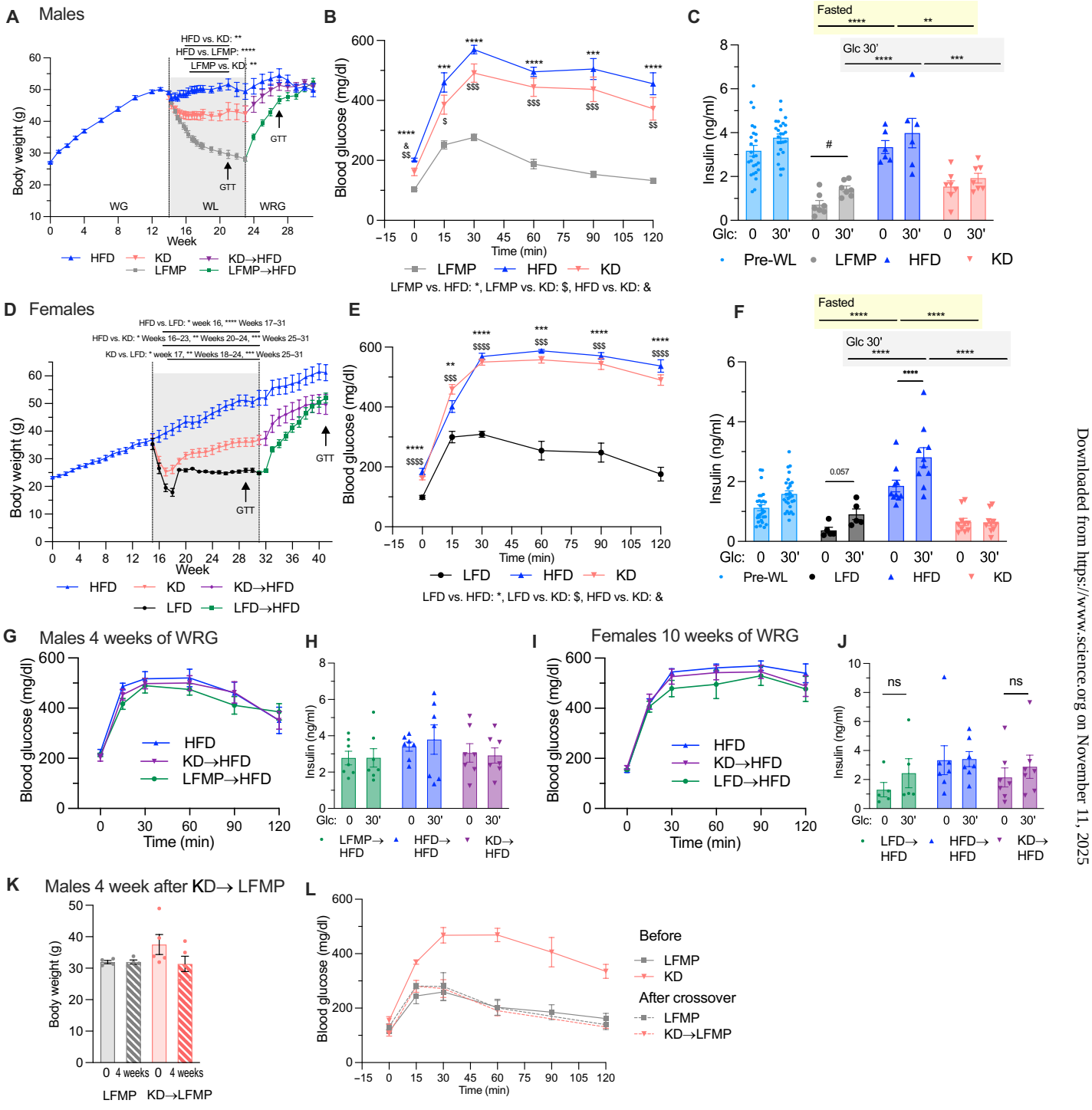

Fig. 7. A KD for WL is less effective than a LFD and causes impaired insulin secretion. (**A** and **D**) Body weight during weigh gain (WG), WL, and WRG intervention in males (A) and females (D). (A) 14 weeks of WG on 60% HFD ($n = 30$), followed by 9 weeks of WL on KD (red) or LFMP (gray) ($n = 7$ to 10 per group), and WRG on HFD (KD→HFD, purple and LFMP→HFD, green) in males. (**B**) GTT after 7 weeks of WL [week 21 dotted line on the BW graph in (A)] with glucose (1.5 mg/g). (**C**) In vivo GSIS: Plasma insulin during GTT in (B) and pre-WL. (**D**) Fifteen weeks of WG on 60% HFD ($n = 28$), followed by 16 weeks of WL on KD (red) or LFD (black) ($n = 5$ to 10 per group). At week 31 (16 weeks of WL), females were switched back to HFD (KD→HFD, purple and LFD→HFD, green) leading to WRG. (**E**) GTT after 14 weeks of WL [week 29 dotted line on the BW graph in (D)] with glucose (1.5 mg/g). (**F**) In vivo GSIS: Plasma insulin during GTT in (E) and pre-WL. (**G** and **I**) GTT with glucose (1.5 mg/g) and (**H** and **J**) plasma insulin during GTT (in vivo GSIS) in males after 4 weeks of WRG [dotted line at week 27 in (A); (G) and (H)] and in females after 10 weeks of WRG [dotted line at week 41 in (D); (I) and (J)]. (**K** and **L**) Following a year-long dietary regimen on either LFMP or KD, KD mice were switched to LFMP for 4 weeks. (K) BW before and after switching the diets. (L) GTT [glucose (1.5 mg/g)] before and 4 weeks after switching to LFMP. Statistics: One-way or two-way ANOVA with post hoc Tukey's HSD. Number of symbols represents significance level: *$P < 0.05$, **$P < 0.01$, ***$P < 0.001$, and ****$P < 0.0001$. Data are represented as means ± SEM. ns, not significant.

of lipid homeostasis and may increase the risk of cardiovascular events (*15*).

Our study is one of few long-term KD interventions (almost 1 year) in which mice had ad libitum access to KD without calorie restriction. We incorporated two low fat diets, a standard LFD with 20% kcal from proteins and a LFMP with a lower 10% kcals from proteins that matches KD protein content to control for the potential confounding effects of reduced proteins. Throughout our investigations, we found that the LFD and LFMP produced virtually identical phenotypes, suggesting that the effects of KD are independent of the more moderate protein content and consistent with studies showing that 10% protein is enough to support normal physiology in B6 mice (*42*, *43*). We also included a comparison group on 60% HFD, the gold standard model of diet-induced obesity for which metabolic disturbances are well described and a group on 60% HFD with very low 0.1% carbohydrate. Our study was powered to detect significant differences, and our results were replicated in two to three independent cohorts. We performed extensive characterization of whole-body metabolic parameters, including state of the art, hyperglycemic clamp, dynamic GSIS, and electron microscopy (EM) experiments. Last, we included both sexes and carefully profiled the diet:sex interaction known to affect metabolic outcomes (*44*, *45*). For the most part, the phenotypic effects of KD followed the same patterns in male and female mice, yet interesting differences were observed as discussed below. Our results set the ground for future investigations into the molecular determinants of KD-mediated insulin secretion defects.

Prior research has led to conflicting findings on weight regulation on KDs. In our study, both male and female B6 mice fed a KD ad libitum gained less weight than mice on an obesogenic 60% HFD but more than mice on a LFD. Several rodent studies reported similar prevention of excessive weight gain on a KD as compared to an HFD (*9*, *18*, *20*, *27*). Weight gain between KD and chow fed rodents has led to more discordant results, with several studies describing lower BW under KD (*19*, *22*, *29*, *46*). Two lifelong studies of mice on KD, noted the necessity of restricting caloric intake (*23*) or cycling the KD with a LFD (*9*) to prevent obesity (*9*, *23*), and another 8-week study in middle-aged females also reported using pair feeding to prevent weight obesity (*47*). The long-term duration of our study and differences in diet compositions across studies, for all diets, can all also affect the phenotypic outcomes (*7*, *48*–*50*). Future studies could directly investigate these parameters that were not explored here.

In our study, reduced caloric intake of KD and LFD/LFMP groups compared to HFD can at least partially explain the lower weight, although concomitant changes in energy expenditure were not assessed systematically. During our WL intervention, we observed a marked decrease in food intake during the first couple of weeks that matches the initial drop in weight. However, weight stabilized after mice increased their ad libitum caloric intake to levels that were slightly below mice maintained on HFD, suggesting that food intake was the main driver of weight changes. KD was less effective than chow diets at inducing WL as mice on LFD/ LFMP lost more than double the weight that mice on KD lost. Moreover, KD did not cure obesity but merely cause a transient WL that was reversed upon resumption of an HFD.

Despite being lighter than mice fed a 60% HFD, males and females on KD had significant increases in plasma TGs and NEFA. KD-fed males also show hepatic steatosis and increased plasmatic ALT activity, suggestive of liver dysfunction. Those findings are in agreement with most other studies of KD (*18*, *20*, *22*). With the increasing prevalence of metabolic dysfunction–associated steatohepatitis and especially in people with obesity, the potential of KD to cause or worsen pre-existing hepatic dysfunction is of utmost concern. Unexpectedly, females on KD did not display signs of hepatic lipid deposition nor liver dysfunction, and these conditions were only observed under 60% HFD. Future studies will explore these sexual dimorphisms with the potential to uncover novel biology of hepatic buffering of lipid spill over.

The effect of KD on glucose homeostasis in mice is controversial. Many reports initially pointed at the benefits of KD on glucose homeostasis (*18*, *25*, *33*), yet a number of recent publications report similar negative effects on glucose tolerance to what we observed (*20*, *24*, *29*–*32*). This glucose intolerance was observed using multiple KDs with varying fat compositions such as with: (i) an 89% kcal fat KD with fat from roughly equal amount of lard and cocoa butter [1% kcal carb, 10% kcal protein; (*30*)], (ii) an 89.5% kcal fat KD with fat from Primex [0.1% kcal carbohydrate, 10.4% kcal protein; Research Diets, D12369B; (*24*)], (iii) an 93.1% kcal fat KD with equal amounts of saturated, monounsaturated, and polyunsaturated fats [1% kcal carb, 5.9% kcals protein; (*31*)], (iv) an 91% kcals fat KD from mostly lard (0% kcal carbohydrate, 9% kcal protein; (*32*)], and (v) an 95.1% kcal fat KD with fat from lard and butter fat [0.4% kcal carbohydrate and 4.5% kcal protein; Bio-Serv (F3666) (*20*, *29*)].

Another shared feature of these KD diets is their very low carbohydrate content (less than 1% kcal). To test the effect of the limited 0.1% sugar content on glucose tolerance, we used a 60% HFD, with identical fat composition to that of the 60% HFD but with a very low 0.1% kcal carbohydrate content (HFHP; 60% kcal fat, 0.1% kcal carbohydrate, and 39.9% kcal protein). This diet uncovered metabolic phenotypes that were largely similar to our KD, with weight gain, glucose intolerance, and impaired insulin secretion, in the absence of elevated circulating KBs. These results suggest that the combined high-fat very-low-carbohydrate nature of KDs, rather than the ketogenic effects per se, likely play a large role in inducing glucose intolerance and islet dysfunction. Hence, it is likely that glucose homeostasis would be dysregulated under many KDs regardless of the specific macronutrient content.

In our study, in vivo GSIS revealed a lack of insulin secretion in KD-fed mice in contrast to LFD and HFD groups. Reviewing the literature highlighted that regardless of the positive or negative effects of KD on GTT, insulin levels in KD mice were low across the board, irrespective of diet composition, age, or study duration (*18*, *19*, *46*, *51*). While this is often pointed to as a positive effect (i.e., prevention or reversal of hyperinsulinemia), we posit that low-insulin levels on a KD are a hallmark of β cell dysfunction and can lead to other detrimental metabolic effects. Accordingly, two prior studies described reduced β cell mass as a cause of low insulin levels (*30*, *31*). In our study, however, extensive characterization of islets mass did not point at differences in islets mass as the underlying determinants of KD-linked insulin secretion defect.

Hyperglycemic clamp further uncovered inefficient rapid insulin secretion in KD-fed mice, a phenomenon that has not been described to the best of our knowledge. In mice on KD, insulin levels did not rise significantly until 90 min into the 120-min clamp study while mice on HFD and KD had an immediate rise in plasma insulin that peaked at 15 min. The exocytosis of insulin containing secretory granules docked at the plasma membrane (*40*, *52*) is incriminated in the early insulin response to glucose, suggesting that this population of insulin granules may be specifically affected by a KD. To assess

cell autonomous defects in insulin secretion, β cells were isolated and tested in an ex vivo dynamic GSIS assay. Both HFD and KD islets had reduced insulin secretion under high glucose compared to LFD islets. Upon KCl-induced depolarization, HFD islets secreted significantly more insulin suggestive of impaired glucose sensing. In contrast, islets from KD-fed mice released similarly low levels of insulin whether stimulated by glucose or KCl, indicating defective insulin secretory machinery.

Integrating in vivo and ex vivo insulin results further highlighted the differences in islets physiology between HFD- and KD-fed mice. Despite the impaired glucose sensing and insulin secretion of isolated islets, HFD-fed mice were hyperinsulinemic and able to secrete insulin during the hyperglycemic clamp. This ability to secrete high levels of insulin in vivo suggests a compensation for cell autonomous defects, which may be linked to islet hyperplasia since mice on HFD have double the number of the largest islets and higher pancreatic insulin content compared to LFD and KD mice. This effect was not assessed in the ex vivo GSIS because islets size was controlled for. It is also very possible that the extracellular milieu influences insulin secretory response in vivo. In particular, islets from KD-fed mice are exposed to a milieu richer in lipids (both NEFA and TG) than HFD islets, and the effects of this milieu are likely abated in our ex vivo GSIS studies. A number of in vitro studies have established a causal link between long-term fatty acid treatment and reduced GSIS (*53*–*55*); however, a washout period has been shown to repair GSIS (*55*). Hence, removing KD islets from their lipotoxic milieu might have improved their insulin secretion in the ex vivo GSIS.

Transcriptomics analysis highlighted alterations in translation, protein transport, Golgi function, and ER/Golgi stress specific to KD islets. Pathways and genes associated with ER transport, COPI and II transport, and secretion from the Golgi were all elevated suggesting increased protein transport pre-Golgi. The transcriptional repression of Rab30 and Rab39, which are important for Golgi organization (*38*, *39*, *56*), suggested Golgi disorganization, and repression of Rab8b impaired Golgi vesicle secretion. From these data, we suggest a model in which Golgi-related defects lead to a traffic jam of proteins in the Golgi and a compensatory upregulation of pre-Golgi transport. ER/Golgi stress markers were also up-regulated under KD. For instance, *Creb3l3*, an ER/Golgi stress marker (*57*), was the most up-regulated gene in KD islets. CREB3 (of the same family as Creb3l3) is up-regulated by palmitate in human β cells where it attenuates palmitate toxicity and is hypothesized to act as a mediator of the Golgi stress response (*58*). Overall, we speculate that high lipids on KD lead to the development of a lipotoxicity stress, which has previously been shown to cause ER stress and disrupt ER to Golgi protein transport in islets (*59*, *60*). Electron microscopy images further confirmed aberrations in the Golgi that appeared dilated and vesiculating in mice on a KD. A recent study characterized the disrupted protein trafficking observed in islets of diabetic leptin receptor KO db/db mice and uncovered distended and vesiculated Golgi very similar to what we see in our KD mice (*61*). Misfolded proinsulin released from the ER is put forth as cause of Golgi dilation and altered morphology (*61*). Incidentally, misfolded proinsulin has been suggested to occur in early stages of type 2 diabetes (T2D) (*62*), so it is possible that increases in misfolded proinsulin cause Golgi swelling and further impair insulin trafficking and secretion.

Overall, we propose that extremely high-lipid levels under KD lead to ER/Golgi stress in islets, thereby disrupting protein trafficking and causing a traffic jam of vesicles in the Golgi. With impaired protein transport and ER stress, the pool of readily releasable insulin available may be insufficient for the islets to rapidly secrete insulin in response to glucose, thus leading to the observed glucose intolerance. It has been postulated that, early on, lipotoxicity induces an expansion of β cell that precedes β cell failure (*63*). We hypothesize that the extra high fat of a KD as compared to an HFD causes mice on KD to bypasses the islet proliferative phase as observed in HFD-fed mice and go straight to early β cell failure. Future experiments will be conducted to test this hypothesis.

Many studies have shown that a KD can lower insulin levels in humans (*64*–*68*) and mice (*19*, *46*), and while this is generally taken as a sign of improved glycemic control and remission of diabetes, our results led us to question whether low-insulin levels are safe and whether they actually indicate improved glycemic control. Insulin is crucial not only for glucose regulation but also for lipid homeostasis through stimulation of plasma lipid clearance and inhibition of lipolysis (*69*–*71*). Insulin resistance is accompanied by elevated blood lipids and ectopic lipid deposition (*72*, *73*), as observed in HFD-fed mice. These metabolic alterations were also observed in KD-fed mice, suggesting that their very low levels of insulin might be insufficient to suppress lipolysis and promote the uptake and benign storage of the excess dietary fat in adipose tissues. Thus, while the lack of insulin on a KD may lead to a lower BW and less fat storage, it may worsens metabolic health by destabilizing lipid homeostasis.

While our findings show that a KD both prevents and causes WL, a KD does not lead to permanent reductions in BW and, thus, should not be treated as a "cure" for obesity or diabetes. Moreover, we observed worsening glucose intolerance and impaired insulin secretion the longer the animals had been on KD, so the vision of KD as a treatment for metabolic disease should be questioned even if initial improvements in health are observed. Although we found that glucose intolerance caused by a KD is reversible, it is possible that other effects may persist. Moreover, in mice with diet-induced obesity, a traditional high-carbohydrate LFD caused greater WL than a KD while improving glucose intolerance.

KD is used to manage refractory epilepsy in children. It is rarely a lifelong intervention as confirmed by a metanalysis of 45 studies reporting that, of children put on a KD, only 45% remain on the diet after 1 year and 29% after 2 years (*74*). Moreover, an international consensus group statement recommends discontinuing KD by 2 years with some experts recommending discontinuation by 6 months (*2*). Because KD is predominantly used in children and discontinued after a short time, long-term studies of metabolic effects are generally lacking. Nevertheless, high-plasma lipids, pancreatitis, and cardiac complications have been reported in patients on KD (*2*, *13*, *15*, *75*–*78*). Studies around the world have also reported higher than average prevalence of diabetes in people with epilepsy (*79*–*81*). The reasons for this co-occurrence are unclear (*82*, *83*), but one hypothesis is that epilepsy treatments increase the likelihood of diabetes (*84*).

In summary, while a KD can prevent and treat obesity, it causes hyperlipidemia, hepatic steatosis, and glucose intolerance. Unlike mice on HFD, the mice on KD do not have detectable insulin resistance or hyperinsulinemia. Instead, they have impairments in insulin secretion due to a blockade in protein trafficking resulting from dilation of the Golgi apparatus, which also causes ER/Golgi stress.

Our study shows that while C57BL/6J male and female mice on a KD are protected from weight gain as compared to mice on a traditional 60% HFD, the mice experience severe glucose intolerance,

high plasma lipids, and impaired insulin secretion with males also developing hepatic steatosis. Further studies in other strains of mice, other animal models, and in humans are necessary to determine whether KD-linked metabolic derangements are universal. Because the KD is not a standardized diet, it has been suggested that saturated versus unsaturated fats and different macronutrient compositions can lead to different metabolic outcomes. While we were able to replicate our results in a group of mice on another type of low-carbohydrate, HFD, future studies to elucidate whether the type of fat and macronutrient composition of the KD influences the metabolic outcomes will be important for making KD safer for all including those who require a KD to treat their epilepsy. Despite these limitations, our findings have relevant translational ramifications. They suggest that a KD used as a long-term dietary intervention may have harmful effects on metabolic health—especially in terms of β cell function, plasma lipid levels, and liver health—and caution against the systematic use of a KD as a health promoting dietary intervention.

MATERIALS AND METHODS

Mice

All animal experiments were carried out in accordance with the guidelines and approved by the Institutional Animal Care and Use Committee (IACUC) of the University of Utah (protocol 1764 to A.C.). C57Bl6/J male and female mice from The Jackson Laboratory (catalog no. 000664) were used in all studies. After receiving mice from Jax, they were placed on chow and allowed to acclimate for at least 3 weeks. When mice were 14 to 15 weeks old, they were placed on their respective diets. Mice had 24-hour ad libitum access to food and water and were on a 12-hour light/12-hour dark cycle. Lights on a 7:00 a.m. Th prevention studies (Figs. 1 to 6) used169 males from three independent cohorts and 60 females from two independent cohorts. The WL studies (Fig. 7) used 30 female and 30 male mice. The male WL study was repeated in two additional cohorts.

Diets

All diets used in the studies were ordered from Research Diets: LFD [10% kcal from fat, 70% kcal from carbohydrates, 20% kcal from protein (D12450K)]; LFMP [10% kcal from fat, 80% kcal from carbohydrates, and 10% kcal from protein (D21110806)]; HFD [60% kcal from fat, 20% kcal from carbohydrates, and 20% kcal from protein (D12492)]; KD [89.9% kcal from fat, 0.1% kcal from carbohydrates, and 10% kcal from protein (D16062902)]; and HFHP [60% kcal from fat, 0.1% kcal from carbohydrates, and 39.9% kcal from protein (D05022501)].

Body composition

Body composition was measured using a Bruker Minispec small animal NMR (Bruker, catalog no. LF50). Animals were awake and freely moving. Measurements were taken during the dark cycles, and animals were in the ad libitum fed state.

Blood glucose and blood ketone beta-hydroxybutyrate

Blood glucose and blood ketone beta-hydroxybutyrate were collected using handheld meters. Venous blood was obtained via a small nick in the tail. Blood glucose meters (Amazon, Nova Max Plus) had a range of 20 to 600 mg/dl, so any readings that were high were given a numeric value of 600. Ketone body meters (Amazon, KetoneBM) measured only the presence of beta-hydroxybutyrate.

GTT and ITT

Before studies, mice were fasted over night for roughly 15 hours. Blood glucose levels were measured at baseline and then at regular intervals during the study as noted. Mice were given intraperitoneal injections of glucose (1.5 mg/g; Sigma-Aldrich, D-(+)-glucose, catalog no. G7021) or insulin (0.75 IU/ kg; Lily Medical, Humulin R U-100) in phosphate-buffered saline (PBS). Blood glucose and blood were collected as noted in the experiment. For in vivo GSIS, blood was collected using a cheek bleed before and during the GTT.

Plasma metabolites

All blood metabolite measures were performed using plasma collected from the submandibular vein. Fed blood was collected in the ad libitum fed state during the middle of the dark cycle (12 p.m.), and fasted blood, which was taken to measures baseline insulin during in vivo GSIS, was collected at 7 a.m. (onset of the dark cycle) following a 14-hour overnight fast. Blood was collected in EDTA tubes (Sarsdtet,16.444.100) and placed immediately on ice. Blood was then spun at 1000*g* for 10 min. Cholesterol, TGs, and nonesterified fatty acids were measured using colorimetric kits (Sekisui Diagnostics, TG: Cat#236–60, Chol: Cat#234–60, NEFA: Cat#s:999–34691, 991–34891, 995–34791, 993–35191, 997–76491). Insulin was measured using an insulin ELISA (Crystal Chem, Cat#90080).

Liver TGs

Liver was collected at sacrifices and immediately snap frozen. Tissues were homogenized using a mortar and pestle kept cold with dry ice and liquid nitrogen. Lipids were extracted using a modified Folch methods. Liver (50 mg) was extracted in 2:1 chloroform:methanol mixture (chloroform: Sigma-Aldrich, C2432-1L). Methanol mixture was vortexed and left at 60°C for 30 to 60 min. The aqueous layer was transferred to a new tube, and 125 μl of water was added for every 500 μl of chloroform/methanol mixture. The mixture was vortexed and then spun at 500*g* for 10 min to cause phase separation. The lower organic layer was moved to a new and liquid was evaporated. Chloroform was added back to resuspend the lipids (20:1 ratio original tissue weight to chloroform). Chloroform mixture (100 μl) was combined with 200 μl of 1% Triton-100 and re-evaporated at 45°C. The leftover lipid triton mix was resuspended in water. Triglycerides were measured using the same TG kit as for the plasma (Sekisui Diagnostics, catalog no. 236-60).

Hyperglycemic clamp

Surgery

Mice were anesthetized using isoflurane (Vet One NDC,13985-528-60; Kent Scientific Somnosuite, 22-01), given anesthetics, and skin was shaved and prepped with betadine and isopropyl alcohol. A small incision was made starting from halfway between the left armpit and midline and extended up roughly 50 cm to the next. The jugular vein was isolated and the catheter (Instech, C20PU-MJV2013) was introduced into 1- to 2-mm incision in the jugular. The catheter was slid roughly 10 mm into the vein, and ligatures (Fine Science Tools, catalog no. 18030-60) were applied above and below catheter insertion to hold it in place. The catheter was then threaded around the side of the mice and pulled through a small incision sitting atop the scapula. Incisions were sutured closed (Covidien, SN1955), The catheter was held in place using a backpack harness (Instech, catalog no. CIH62) and filled with lock solution. Mice were allowed to recover for 4 days.

Clamp procedure

On the day of the study catheters were connected to a swivel system (Instech, catalog no. KVAH62T), allowing mice to be freely moving during the clamp. Blood glucose was measured beginning 90 min before the clamp to ensure mice had a steady baseline glucose. Mice were infused with 50% glucose in saline starting at a rate of 500 μl/hour for 2 min. After the first 2 minutes, the infusion rate was changed to an amount in microliters that was 3× the BW (is a 50 g of mouse received an infusion of 150 μl/hour). Then, the infusion amounts were changed on the basis of BG levels that were taken every 3 to 5 min with a target glucose level of 250 mg/dl. Tail bleeds were also performed at baseline 0, 5, 10, 15, 20, 25, 30, 60, 90, and 120 so that insulin levels could be measured.

Islet harvest for RNA sequencing

Mouse was euthanized, and the pancreas was perfused using an oxygenated buffer of Hanks' balanced salt solution (HBSS) (Thermo Fisher Scientific, catalog no. 14025092) with 25 mM Hepes (Gibco, catalog no. 15630-080), 8 mM glucose, and 0.2% bovine serum albumin (BSA). Liberase (0.1 mg/ml; Sigma-Aldrich, 0540102001) was added tto the buffer for pancreas digestions. The pancreas was digested at 37°C for 30 min. After 30 min, the samples were flooded with fresh buffer and allowed to settle for 10 min, so that the islets would sink to the bottom and the debris would float to the top; part of the supernatant was removed, fresh buffer was added to replace the volume removed, and samples were agitated to mix. This process was repeated until the liquid was very clear (four to six times); the islets with the clear liquid were then handpicked under a microscope. Islets were then pelleted, washed with PBS, and snap frozen.

RNA sequencing and analysis

RNA was extracted using TRIzol (Invitrogen, catalog no. 15596018) chloroform and followed by a QIAGEN RNEasy kit with deoxyribonuclease treatment (Islets: micro kit 74004; liver: Mini Kit 74106). The University of Utah High Throughput Genomics core performed RNA sequencing with the following methods. Total RNA samples (5 to 500 ng) were hybridized with NEBNext rRNA Depletion Kit v2 (human, mouse, and rat) (E7400) to substantially diminish ribosomal RNA from the samples. Stranded RNA sequencing libraries were prepared as described using the NEBNext Ultra II Directional RNA Library Prep Kit for Illumina (E7760L). Purified libraries were qualified on an Agilent Technologies 4150 TapeStation using a D1000 ScreenTape assay (catalog no. 5067-5582 and 5067-5583). The molarity of adapter-modified molecules was defined by quantitative PCR using the Kapa Biosystems Kapa Library Quant Kit (catalog no. KK4824). Individual libraries were normalized and pooled in preparation for Illumina sequence analysis. The following adapter reads were used: *Adapter Read1* (AGATCGGAAGAGCACACGTCTGAACTCCAGTCA) and *Adapter Read 2* (AGATCGGAAGAGCGTCGTGTAGGGAAAGAGTGT). Sequencing libraries were chemically denatured in preparation for sequencing. Following transfer of the denatured samples to an Illumina NovaSeq X instrument, a 150 × 150 cycle paired-end sequence run was performed using a NovaSeq X Series 10B Reagent Kit (20085594). Data were aligned to mm39, and deseq2 analysis was run as described by Love *et al.* (*85*) by the University of Utah Bioninformatics Core. Pathway analysis was performed using Reactome (*86*) camera analysis on DE genes. Metascape (*87*) was also run on DE genes to identify gene ontology groups that were enriched. UpSet (*88*) plots were used for data visualization.

Fastq files are available online: Liver RNA sequencing [gene expression omnibus (GEO): GSE248297 (www.ncbi.nlm.nih.gov/geo/query/acc.cgi?acc=GSE248297)] and Islet RNA sequencing (GEO: GSE268020; www.ncbi.nlm.nih.gov/geo/query/acc.cgi?acc=GSE268020). The data will be ready and available to the public before publishing.

Insulin staining and islet sizing

Pancreas was collected after 29 weeks on the respective diets from both male and female mice. In males, 8 to 12 slices were taken throughout the entire pancreas from $n = 4$ to 6 animals per groups for a total 5157 islets analyzed on LFD, 6718 on HFD, and 6389 on KD. For females, six and seven slices were taken throughout the entire pancreas ($n = 5$ per group), for a total of 3749 LFMP, and 3428 KD islets were analyzed.

Sections for histology were collected at sacrifice and then placed in 10% formaldehyde (Ricca, catalog no. 3190-5) for 24 hours, followed by 70% ethanol (Decon Laboratories, catalog no. 2701). Sections were then paraffin embedded and sectioned to 5-μm thickness by the University of Utah Research Histology Core. Sections were deparrafinized and rehydrated in sequential 3-min soaks in xylene (2×) (Sigma-Aldrich, catalog no. 296325), 100% ethanol (Decon Laboratories, catalog no. 2701), 95% ethanol, 70% ethanol, 50% ethanol, and water. Antigen retrieval was performed using 10 mM sodium citrate (Thermo Fisher Scientific, BP327-500) with 0.05% Tween 20 (Calbiochem, 655204) pH 6 in kept around 95°C for 30 min. A 30- to 60-min blocking step with 2% BSA (Sigma-Aldrich, catalog no. A7906) in tris-buffered saline was performed, followed by 30% incubation with 3% hydrogen peroxide to quench endogenous peroxidase activity. After washing 3× for 5 min with PBS + 0.05% Tween 20 the horseradish peroxidase–conjugated insulin antibody was used (Abcam, catalog no. 28063 mouse anti-insulin and pro-insulin- AB dilution, 1:200) in the dark for 60 min. Antibody was washed off as described above and followed DAB application (Thermo Fisher Scientific, catalog no. 34002) and a hematoxylin counterstain (Vector Labs, catalog no. H-3502). Slides were then dehydrated and coverslipped. Slides were imaged on an Axioscan 7 slide scanner (Zeiss), and images were processed in Qupath (*89*). To quantify insulin positive area, thresholding for DAB staining was performed, and manual corrections were made as needed to remove artifacts or add islets that were not counted. A minimum islet size was set to exclude islets with an area of less than 100 μm^2; this corresponds to a diameter of roughly 11.28 μm, which is slightly larger than a singular β cell, and detections smaller than 100 μm^2 often did not contain a visible nucleus. We calculated area and perimeter for each unique islet. A separate analysis in Qupath for total pancreas area was created. We created a positive area detection threshold for hematoxylin and measured the total area; regions of adipose tissue surrounding the pancreas were removed. Area and perimeter data for islets and the pancreas sections were extracted from Qupath. The binned areas used in the frequency distribution correspond to islet diameter as follows: 100 μm^2 = diameter of 11.3 μm or the size one β cell (and the minimum size needed to identify a nucleus and clear borders in the analysis); 170 μm^2 = diameter of 14.7 μm; 490.87 μm^2 = diameter of 25 μm; 1963 μm^2 = diameter of 50 μm; 4417.86 μm^2 = diameter of 75 μm; 7853.981 μm^2 = diameter of 100 μm; and 17,671 μm^2 = diameter of 150 μm.

Liver histology and scoring

Sections for histology were collected at sacrifice and then placed in 10% formaldehyde (Ricca, catalog no. 3190-5) for 24 hours,

followed by 70% ethanol (Decon Laboratories, catalog no. 2701). Sections were then paraffin embedded, sectioned to 5-μm thickness, and stained with H&E by the University of Utah Research Histology Core. Slides contained one section from each diet group and were scored by a board-certified pathologist (K.J.E.) who was blinded to the diet conditions. Steatosis was determined by estimating percent area containing lipid droplets, and liver inflammation was scored between 0 and 3 based on the scale developed by Liang *et al.* (*90*). Images were acquired using cellSens software and an Olympus DP73 camera attached to an Olympus BX53 microscope with UPlanFL objectives.

Electron microscopy

Mice were anesthetized by isoflurane gas. Mice were anesthetized using isoflurane (Vet One, NDC,13985-528-60; Kent Scientific Somnosuite, 22-01) and fixed by cardiac perfusion with 2.5% glutaraldehyde and 1% paraformaldehyde, 6 mM $CaCl_2$, and 2.4% sucrose in 0.1 M cacodylate buffer (pH 7.4; Electron Microscopy Sciences, catalog no. 16537-07). Immediately after perfusion, the pancreas was dissected out and soaked in fresh fixative, where the organ was sliced into small blocks of about 10 mm^3. Tissue blocks were transferred into fresh fixative where they were continuously fixed for at least 2 hours at room temperature before being stored at 4°C. Sample processing and conventional electron microscopy were conducted by the University of Utah Electron Microscopy Core Facility using a microwave-assisted fixation and processing protocol (Pelco Biowave, 36500). Sequential steps were as follows: 2% osmium post-fixation, 4% uranyl acetate en-bloc staining, serial dehydration in ethanol/acetone, and embedding in Embed 812 (Electron Microscopy Sciences, catalog no. 14120). Specimens in the cured epoxy-resin block was sectioned using Lecia ultramicrotome UC6. The islet of Langerhans was identified under a light microscope in semithin sections stained with toluidine, then ultrathin sections of 100-nm thickness were cut and deposited onto carbon-formvar–coated slot grids. Sections on grids were further contrast-stained with uranyl acetate and lead citrate and examined at 120 kV with JEOL JEM 1400 equipped with a GatanOrius digital camera.

Whole pancreas insulin quantification

At sacrifice, pancreas was carefully dissected and weighed. A small piece (10 to 20 mg) was taken and weighed separately. This small piece was added to a tube containing 5 ml of acid ethanol extraction buffer (1.5 ml of 1 N HCl with 98.5 ml of 70% ethanol). The pancreas was homogenized by vortexing with metal screws for 2 hours on two consecutive days or until mixture was homogenized. The slurry was then centrifuged at 2000*g* for 3 min to pellet any debris. A 500 ml of supernatant was mixed with 500 ml of 1 M tris. The tris extract mixture was then diluted 1:100 using Crystal Chem Islet sample diluent and then run on the Crystal Chem ELISA using the high range assay.

Ex vivo GSIS

The ex vivo GSIS was performed by the Vanderbilt islet and pancreas core using established protocol that are found online: islet harvest (*91*) and islet perifusion (*92*).

Islet harvest

Mice were anesthetized with ketamine/xylazine solution (1 μl/mg BW), and after the loss of consciousness, they were placed on a surgical stage and skin was prepped with 70% ethanol. The skin and peritoneum were opened, and the bile duct was located and closed with a suture at the duodenum. Using a bent 30-gauge needle collagenase solution [collagenase P (0.6 mg/ml) in HBSS] (collagenase: MilliporeSigma, catalog no. 11249002001; HBSS: Thermo Fisher Scientific, catalog no. 14025) was injected into the bile duct entering the duct near the liver to inflate the pancreas. The pancreas was removed and placed in a conical tube containing 5 ml of HBSS/collagenase solution, and the tubes were placed in a 37°C water bath shaker for 8 min with shaking by hand every 4 min and until the tissue had dissolved into a slurry at the end of the second shaking. Tubes were placed on ice and topped up to 15 ml with HBSS with 10% FBS (Sigma-Aldrich, catalog no. F0926) and then centrifuged at 200 rcf for 00:01:00 at 25°C. Liquid was decanted, and pellets were washed by adding 10 ml of HBSS with 10% FBS and then vortexed to mix before centrifuging again. This process was repeated 3×. After the final wash, supernatant was discarded, and 10 ml of HBSS with 10% FBS was added and mixed. The slurry was transferred to a 50-ml conical tube. The original tube was washed with another 5 ml of HBSS with 10% FBS and added to the 50-ml tube for a total of 15 ml of digest. The digest was vortexed, and 15 ml of Histopaque gradient was underlayed using a manual bulb pipette. Tubes were centrifuged at 500 rcf for 00:10:00 at 25°C. New 50-ml tubes containing 15 ml of HBSS with 1% FBS were prepared, and islet layer was transferred to the new tubes. Tubes were centrifuged tubes at 500 rcf for 00:10:00 at 25°C, the liquid was decanted, and pellets were washed 3× with 25 ml of HBSS with 1% FBS vortexing each time after adding HBSS to mix before centrifugation. After the final decanting, 10 ml of HBSS with 10% FBS was added to the tube and mixed by pipetting. The mixture was transferred to a 10-cm untreated culture dish. Islets were handpicked under an inverted microscope at 4×. Islets were then sized and handpicked to a 6-cm dish.

Perifusion

Base perifusion media: 1 liter of deionized water plus the following: 3.2 g of $NaHCO_3$ (Sigma-Aldrich, catalog no. S6014-500G), 0.58 g of L-glutamine (Sigma-Aldrich, catalog no. G8540-100G), 0.11 g of sodium pyruvate (Sigma-Aldrich, catalog no. P2256-25G), 1.11 g of Hepes (Sigma-Aldrich, catalog no. H7523), 8.28 g of Dulbecco's modified Eagle's medium (Sigma-Aldrich, catalog no. 90113), 1 g of RIA-grade BSA (Sigma-Aldrich, catalog no. A7888), and 70 mg of L-ascorbic acid (Sigma-Aldrich, catalog no. A5960).

Glucose medium (5.6 mM) was made by combining 550 ml of base media with 0.5549 g of glucose (Sigma-Aldrich, catalog no. D16). High-glucose medium (16.7 mM) was made by adding 0.7522 g of glucose (Sigma-Aldrich, catalog no. D16) to 250 ml of base perifusion medium. KCl medium was mice by by adding 0.149 g of potassium chloride (Sigma-Aldrich, catalog no. BP366-500) to 100 ml of 5.6 mM glucose media. Perifusion setup was made up of a circulating water bath, a fraction collector, a peristaltic pumps capable of pumping 1 ml/min, and glass columns with two fixed-end pieces (Diba Omnifit LC columns (Cole Parmer, catalog no. 006CC-10-05-FF) as described (*92*).

Islets were transferred to a clear 1.5-ml microcentrifuge tube and then loaded into perifusion system. Bubbles were removed, before starting the system, and fraction collection was set to every 3 min. After collection of 10 preliminary fractions using 5.6 mM glucose baseline media to wash the islets, the experiment started. Baseline medium was used from 0 to 12 min, 16.7 mM glucose medium was used from 12–42 minutes, and then intake was switched back to

baseline media from 42 to 63 min. Next, 5.6 mM glucose with 20 mM KCl was used from 63 to 72 min, and then the medium was switched back to the baseline media for the rest of the experiment. Islets were recovered to a 6-cm dish to calculate IEQ after the perifusion.

Quantification and statistical analysis

Graphpad Prism was used for all statistical analyses. A P value of ≤ 0.05 was used as the cutoff for significance. All results and tests used can be found in the relevant figure and figure legends. Graphs show all individual data points with the bar showing the mean and the error bars showing SEM. One-way or two-way analysis of variance (ANOVA) were used for all group comparisons with post hoc Tukey's HSD test aside from sequencing, which used Deseq2 analysis and a Benjamini-Hochberg correction for the adjusted P value. Sample sizes were determined with a power calculation, and animals were randomly assigned to groups that were matched for BW and spread.

Supplementary Materials

This PDF file includes:

Figs. S1 to S7

REFERENCES AND NOTES

1. A. Paoli, A. Rubini, J. S. Volek, K. A. Grimaldi, Beyond weight loss: A review of the therapeutic uses of very-low-carbohydrate (ketogenic) diets. *Eur. J. Clin. Nutr.* **67**, 789–796 (2013).
2. E. H. Kossoff, B. A. Zupec-Kania, P. E. Amark, K. R. Ballaban-Gil, A. G. C. Bergqvist, R. Blackford, J. R. Buchhalter, R. H. Caraballo, J. H. Cross, M. G. Dahlin, E. J. Donner, J. Klepper, R. S. Jehle, H. D. Kim, Y. M. C. Liu, J. Nation, D. R. Nordli Jr., H. H. Pfeifer, J. M. Rho, C. E. Stafstrom, E. A. Thiele, Z. Turner, E. C. Wirrell, J. W. Wheless, P. Veggiotti, E. P. G. Vining, Charlie Foundation, Practice Committee of the Child Neurology Society, Practice Committee of the Child Neurology Society, International Ketogenic Diet Study Group, Optimal clinical management of children receiving the ketogenic diet: Recommendations of the International Ketogenic Diet Study Group. *Epilepsia* **50**, 304–317 (2009).
3. I. D'Andrea Meira, T. T. Romão, H. J. P. do Prado, L. T. Krüger, M. E. P. Pires, P. O. da Conceição, Ketogenic diet and epilepsy: What we know so far. *Front. Neurosci.* **13**, 5 (2019).
4. A. L. Hartman, M. Gasior, E. P. G. Vining, M. A. Rogawski, The neuropharmacology of the ketogenic diet. *Pediatr. Neurol.* **36**, 281–292 (2007).
5. N. N. Danial, A. L. Hartman, C. E. Stafstrom, L. L. Thio, How does the ketogenic diet work? Four potential mechanisms. *J. Child Neurol.* **28**, 1027–1033 (2013).
6. A. M. Hassan, D. L. Keene, S. E. Whiting, P. J. Jacob, J. R. Champagne, P. Humphreys, Ketogenic diet in the treatment of refractory epilepsy in childhood. *Pediatr. Neurol.* **21**, 548–552 (1999).
7. A. Paoli, Ketogenic diet for obesity: Friend or foe? *Int. J. Environ. Res. Public Health* **11**, 2092–2107 (2014).
8. T. J. W. McDonald, M. C. Cervenka, Lessons learned from recent clinical trials of ketogenic diet therapies in adults. *Curr. Opin. Clin. Nutr. Metab. Care* **22**, 418–424 (2019).
9. J. C. Newman, A. J. Covarrubias, M. Zhao, X. Yu, P. Gut, C.-P. Ng, Y. Huang, S. Haldar, E. Verdin, Ketogenic diet reduces midlife mortality and improves memory in aging mice. *Cell Metab.* **26**, 547–557.e8 (2017).
10. S.-J. Wei, J. R. Schell, E. S. Chocron, M. Varmazyad, G. Xu, W. H. Chen, G. M. Martinez, F. F. Dong, P. Sreenivas, R. Trevino, H. Jiang, Y. Du, A. Saliba, W. Qian, B. Lorenzana, A. Nazarullah, J. Chang, K. Sharma, E. Munkácsy, N. Horikoshi, D. Gius, Ketogenic diet induces p53-dependent cellular senescence in multiple organs. *Sci. Adv.* **10**, eado1463 (2024).
11. S. Joshi, R. J. Ostfeld, M. McMacken, The ketogenic diet for obesity and diabetes-enthusiasm outpaces evidence. *JAMA Intern. Med.* **179**, 1163–1164 (2019).
12. M. Watanabe, D. Tuccinardi, I. Ernesti, S. Basciani, S. Mariani, A. Genco, S. Manfrini, C. Lubrano, L. Gnessi, Scientific evidence underlying contraindications to the ketogenic diet: An update. *Obes. Rev.* **21**, e13053 (2020).
13. P. O. Kwiterovich Jr., E. P. Vining, P. Pyzik, R. Skolasky Jr., J. M. Freeman, Effect of a high-fat ketogenic diet on plasma levels of lipids, lipoproteins, and apolipoproteins in children. *JAMA* **290**, 912–920 (2003).
14. H. C. Kang, D. E. Chung, D. W. Kim, H. D. Kim, Early- and late-onset complications of the ketogenic diet for intractable epilepsy. *Epilepsia* **45**, 1116–1123 (2004).
15. M. Budoff, V. S. Manubolu, A. Kinninger, N. G. Norwitz, D. Feldman, T. R. Wood, J. Fialkow, R. Cury, T. Feldman, K. Nasir, Carbohydrate restriction-induced elevations in LDL-cholesterol and atherosclerosis: The KETO trial. *JACC Adv.* **3**, 101109 (2024).
16. A. Merovci, B. Finley, A. Hansis-Diarte, S. Neppala, M. A. Abdul-Ghani, E. Cersosimo, C. Triplitt, R. A. DeFronzo, Effect of weight-maintaining ketogenic diet on glycemic control and insulin sensitivity in obese T2D subjects. *BMJ Open Diabetes Res. Care* **12**, e004199 (2024).
17. I. J. Goldberg, N. Ibrahim, C. Bredefeld, S. Foo, V. Lim, D. Gutman, L. A. Huggins, R. A. Hegele, Ketogenic diets, not for everyone. *J. Clin. Lipidol.* **15**, 61–67 (2021).
18. A. R. Kennedy, P. Pissios, H. Otu, B. Xue, K. Asakura, N. Furukawa, F. E. Marino, F.-F. Liu, B. B. Kahn, T. A. Libermann, E. Maratos-Flier, A high-fat, ketogenic diet induces a unique metabolic state in mice. *Am. J. Physiol. Endocrinol. Metab.* **292**, E1724–E1739 (2007).
19. M. K. Badman, A. R. Kennedy, A. C. Adams, P. Pissios, E. Maratos-Flier, A very low carbohydrate ketogenic diet improves glucose tolerance in ob/ob mice independently of weight loss. *Am. J. Physiol. Endocrinol. Metab.* **297**, E1197–E1204 (2009).
20. J. R. Garbow, J. M. Doherty, R. C. Schugar, S. Travers, M. L. Weber, A. E. Wentz, N. Ezenwajiaku, D. G. Cotter, E. M. Brunt, P. A. Crawford, Hepatic steatosis, inflammation, and ER stress in mice maintained long term on a very low-carbohydrate ketogenic diet. *Am. J. Physiol. Endocrinol. Metab.* **300**, G956–G967 (2011).
21. M. M. Poplawski, J. W. Mastaitis, F. Isoda, F. Grosjean, F. Zheng, C. V. Mobbs, Reversal of diabetic nephropathy by a ketogenic diet. *PLOS ONE* **6**, e18604 (2011).
22. N. Douris, T. Melman, J. M. Pecherer, P. Pissios, J. S. Flier, L. C. Cantley, J. W. Locasale, E. Maratos-Flier, Adaptive changes in amino acid metabolism permit normal longevity in mice consuming a low-carbohydrate ketogenic diet. *Biochim. Biophys. Acta* **1852**, 2056–2065 (2015).
23. M. N. Roberts, M. A. Wallace, A. A. Tomilov, Z. Zhou, G. R. Marcotte, D. Tran, G. Perez, E. Gutierrez-Casado, S. Koike, T. A. Knotts, D. M. Imai, S. M. Griffey, K. Kim, K. Hagopian, M. Z. McMackin, F. G. Haj, K. Baar, G. A. Cortopassi, J. J. Ramsey, J. A. Lopez-Dominguez, A ketogenic diet extends longevity and healthspan in adult mice. *Cell Metab.* **26**, 539–546. e5 (2017).
24. E. L. Goldberg, I. Shchukina, J. L. Asher, S. Sidorov, M. N. Artyomov, V. D. Dixit, Ketogenesis activates metabolically protective γδ T cells in visceral adipose tissue. *Nat. Metab.* **2**, 50–61 (2020).
25. T. Okuda, N. Morita, A very low carbohydrate ketogenic diet prevents the progression of hepatic steatosis caused by hyperglycemia in a juvenile obese mouse model. *Nutr. Diabetes* **2**, e50–e50 (2012).
26. K. Oishi, D. Uchida, N. Ohkura, R. Doi, N. Ishida, K. Kadota, S. Horie, Ketogenic diet disrupts the circadian clock and increases hypofibrinolytic risk by inducing expression of plasminogen activator inhibitor-1. *Arterioscler. Thromb. Vasc. Biol.* **29**, 1571–1577 (2009).
27. A. M. Holland, W. C. Kephart, P. W. Mumford, C. B. Mobley, R. P. Lowery, J. J. Shake, R. K. Patel, J. C. Healy, D. J. McCullough, H. A. Kluess, K. W. Huggins, A. N. Kavazis, J. M. Wilson, M. D. Roberts, Effects of a ketogenic diet on adipose tissue, liver, and serum biomarkers in sedentary rats and rats that exercised via resisted voluntary wheel running. *Am. J. of Physiol. Regul. Integr. Comp. Physiol.* **311**, R337–R351 (2016).
28. N. Douris, B. N. Desai, T. Cisu, A. J. Fowler, E. Zarebidaki, N. L. T. Nguyen, D. A. Morgan, T. J. Bartness, K. Rahmouni, J. S. Flier, β-adrenergic receptors are critical for weight loss but not for other metabolic adaptations to the consumption of a ketogenic diet in male mice. *Mol. Metab.* **6**, 854–862 (2017).
29. F. R. Jornayvaz, M. J. Jurczak, H. Y. Lee, A. L. Birkenfeld, D. W. Frederick, D. Zhang, X. M. Zhang, V. T. Samuel, G. I. Shulman, A high-fat, ketogenic diet causes hepatic insulin resistance in mice, despite increasing energy expenditure and preventing weight gain. *Am. J. Physiol. Endocrinol. Metab.* **299**, E808–E815 (2010).
30. T. K. Her, W. S. Lagakos, M. R. Brown, N. K. LeBrasseur, K. Rakshit, A. V. Matveyenko, Dietary carbohydrates modulate metabolic and β-cell adaptation to high-fat diet-induced obesity. *Am. J. Physiol. Endocrinol. Metab.* **318**, E856–E865 (2020).
31. J. H. Ellenbroek, L. van Dijck, H. A. Töns, T. J. Rabelink, F. Carlotti, B. E. P. B. Ballieux, E. J. P. de Koning, Long-term ketogenic diet causes glucose intolerance and reduced β-and α-cell mass but no weight loss in mice. *Am. J. Physiol. Endocrinol. Metab.* **306**, E552–E558 (2014).
32. B. Yau, S. Madsen, M. E. Nelson, K. C. Cooke, A. M. Fritzen, I. H. Thorius, J. Stöckli, D. E. James, M. A. Kebede, Genetics and diet shape the relationship between islet function and whole body metabolism. *Am. J. Physiol. Endocrinol. Metab.* **326**, E663–E672 (2024).
33. A. Weber, K. D. Medak, L. K. Townsend, D. C. Wright, Ketogenic diet induced weight loss occurs independent of housing temperature and is followed by hyperphagia and weight regain after cessation in mice. *J. Physiol.* **600**, 4677–4693 (2022).
34. S. Nasser, T. Solé, N. Vega, T. Thomas, A. Balcerczyk, M. Strigini, L. Pirola, Ketogenic diet administration to mice after a high-fat-diet regimen promotes weight loss, glycemic normalization and induces adaptations of ketogenic pathways in liver and kidney. *Mol. Metab.* **65**, 101578 (2022).
35. A. A. Greenwell, C. T. Saed, S. A. T. Dakhili, K. L. Ho, K. Gopal, J. S. F. Chan, O. O. Kaczmar, S. A. Dyer, F. Eaton, G. D. Lopaschuk, R. A. Batran, J. R. Ussher, An isoproteic cocoa

butter-based ketogenic diet fails to improve glucose homeostasis and promote weight loss in obese mice. *Am. J. Physiol. Endocrinol. Metab.* **323**, E8–E20 (2022).
36. S. A. Amiel, T. Dixon, R. Mann, K. Jameson, Hypoglycaemia in Type 2 diabetes. *Diabet. Med.* **25**, 245–254 (2008).
37. L. Sampieri, P. Di Giusto, C. Alvarez, CREB3 transcription factors: ER-Golgi stress transducers as hubs for cellular homeostasis. *Front. Cell Dev. Biol.* **7**, 123 (2019).
38. B. Goud, S. Liu, B. Storrie, Rab proteins as major determinants of the Golgi complex structure. *Small GTPases* **9**, 66–75 (2018).
39. K. L. Zulkefli, I. S. Mahmoud, N. A. Williamson, P. K. Gosavi, F. J. Houghton, P. A. Gleeson, A role for Rab30 in retrograde trafficking and maintenance of endosome-TGN organization. *Exp. Cell Res.* **399**, 112442 (2021).
40. Z. Fu, E. R. Gilbert, D. Liu, Regulation of insulin synthesis and secretion and pancreatic β-cell dysfunction in diabetes. *Curr. Diabetes Rev.* **9**, 25–53 (2013).
41. M. Omar-Hmeadi, O. Idevall-Hagren, Insulin granule biogenesis and exocytosis. *Cell. Mol. Life Sci.* **78**, 1957–1970 (2021).
42. S. Hu, L. Wang, D. Yang, L. Li, J. Togo, Y. Wu, Q. Liu, B. Li, M. Li, G. Wang, X. Zhang, C. Niu, J. Li, Y. Xu, E. Couper, A. Whittington-Davies, M. Mazidi, L. Luo, S. Wang, A. Douglas, J. R. Speakman, Dietary fat, but not protein or carbohydrate, regulates energy intake and causes adiposity in mice. *Cell Metab.* **28**, 415–431.e4 (2018).
43. Y. Wu, B. Li, L. Li, S. E. Mitchell, C. L. Green, G. D'Agostino, G. Wang, L. Wang, M. Li, J. Li, C. Niu, Z. Jin, A. Wang, Y. Zheng, A. Douglas, J. R. Speakman, Very-low-protein diets lead to reduced food intake and weight loss, linked to inhibition of hypothalamic mTOR signaling, in mice. *Cell Metab.* **33**, 888–904.e6 (2021).
44. L. Brennan, H. Gibbons, Sex matters: A focus on the impact of biological sex on metabolomic profiles and dietary interventions. *Proc. Nutr. Soc.* **79**, 205–209 (2020).
45. Y. Yang, D. L. Smith Jr., K. D. Keating, D. B. Allison, T. R. Nagy, Variations in body weight, food intake and body composition after long-term high-fat diet feeding in C57BL/6J mice. *Obesity* **22**, 2147–2155 (2014).
46. P. Pissios, S. Hong, A. R. Kennedy, D. Prasad, F.-F. Liu, E. Maratos-Flier, Methionine and choline regulate the metabolic phenotype of a ketogenic diet. *Mol. Metab.* **2**, 306–313 (2013).
47. S. J. Pathak, Z. Zhou, D. Steffen, T. Tran, Y. Ad, J. J. Ramsey, J. M. Rutkowsky, K. Baar, 2-month ketogenic diet preferentially alters skeletal muscle and augments cognitive function in middle aged female mice. *Aging Cell* **21**, e13706 (2022).
48. G. S. Neves, M. S. Lunardi, K. Lin, D. K. Rieger, L. C. Ribeiro, J. D. Moreira, Ketogenic diet, seizure control, and cardiometabolic risk in adult patients with pharmacoresistant epilepsy: A review. *Nutr. Rev.* **79**, 931–944 (2020).
49. D. L. Gilbert, P. L. Pyzik, J. M. Freeman, The ketogenic diet: Seizure control correlates better with serum β-hydroxybutyrate than with urine ketones. *J. Child Neurol.* **15**, 787–790 (2000).
50. I. Elisia, M. Yeung, S. Kowalski, T. Shyp, J. Tee, S. Hollman, A. Wong, J. King, R. Dyer, P. H. Sorensen, G. Krystal, A ketogenic diet rich in fish oil is superior to other fats in preventing NNK-induced lung cancer in A/J mice. *Sci. Rep.* **14**, 5610 (2024).
51. S. Schnyder, K. Svensson, B. Cardel, C. Handschin, Muscle PGC-1α is required for long-term systemic and local adaptations to a ketogenic diet in mice. *Am. J. Physiol. Endocrinol. Metab.* **312**, E437–E446 (2017).
52. Z. Wang, D. C. Thurmond, Mechanisms of biphasic insulin-granule exocytosis - roles of the cytoskeleton, small GTPases and SNARE proteins. *J. Cell Sci.* **122**, 893–903 (2009).
53. M. L. Watson, K. Macrae, A. E. Marley, H. S. Hundal, Chronic effects of palmitate overload on nutrient-induced insulin secretion and autocrine signalling in pancreatic MIN6 β Cells. *PLOS ONE* **6**, e25975 (2011).
54. J. Barlow, V. H. Jensen, M. Jastroch, C. Affourtit, Palmitate-induced impairment of glucose-stimulated insulin secretion precedes mitochondrial dysfunction in mouse pancreatic islets. *Biochem. J.* **473**, 487–496 (2016).
55. Y. P. Zhou, V. E. Grill, Long-term exposure of rat pancreatic islets to fatty acids inhibits glucose-induced insulin secretion and biosynthesis through a glucose fatty acid cycle. *J. Clin. Invest.* **93**, 870–876 (1994).
56. S. Liu, B. Storrie, Are Rab proteins the link between Golgi organization and membrane trafficking? *Cell. Mol. Life Sci.* **69**, 4093–4106 (2012).
57. J. H. Reiling, A. J. Olive, S. Sanyal, J. E. Carette, T. R. Brummelkamp, H. L. Ploegh, M. N. Starnbach, D. M. Sabatini, A CREB3–ARF4 signalling pathway mediates the response to Golgi stress and susceptibility to pathogens. *Nat. Cell Biol.* **15**, 1473–1485 (2013).
58. K. E. Rohli, C. K. Boyer, S. E. Blom, S. B. Stephens, Nutrient regulation of pancreatic islet β-cell secretory capacity and insulin production. *Biomolecules* **12**, 335 (2022).
59. Y. S. Oh, G. D. Bae, D. J. Baek, E.-Y. Park, H.-S. Jun, Fatty acid-induced lipotoxicity in pancreatic β-cells during development of Type 2 diabetes. *Front. Endocrinol. (Lausanne)* **9**, 384 (2018).
60. A. M. Preston, E. Gurisik, C. Bartley, D. R. Laybutt, T. J. Biden, Reduced endoplasmic reticulum (ER)-to-Golgi protein trafficking contributes to ER stress in lipotoxic mouse beta cells by promoting protein overload. *Diabetologia* **52**, 2369–2373 (2009).
61. C. K. Boyer, C. J. Bauchle, J. Zhang, Y. Wang, S. B. Stephens, Synchronized proinsulin trafficking reveals delayed Golgi export accompanies β-cell secretory dysfunction in rodent models of hyperglycemia. *Sci. Rep.* **13**, 5218 (2023).
62. A. Arunagiri, L. Haataja, A. Pottekat, F. Pamenan, S. Kim, L. M. Zeltser, A. W. Paton, J. C. Paton, B. Tsai, P. Itkin-Ansari, R. J. Kaufman, M. Liu, P. Arvan, Proinsulin misfolding is an early event in the progression to type 2 diabetes. *eLife* **8**, e44532 (2019).
63. R. B. Sharma, L. C. Alonso, Lipotoxicity in the pancreatic β cell: Not just survival and function, but proliferation as well? *Curr. Diab. Rep.* **14**, 492 (2014).
64. K. A. Meckling, C. O'Sullivan, D. Saari, Comparison of a low-fat diet to a low-carbohydrate diet on weight loss, body composition, and risk factors for diabetes and cardiovascular disease in free-living, overweight men and women. *J. Clin. Endocrinol. Metabol.* **89**, 2717–2723 (2004).
65. J. S. Volek, M. J. Sharman, D. M. Love, N. G. Avery, A. L. Gómez, T. P. Scheett, W. J. Kraemer, Body composition and hormonal responses to a carbohydrate-restricted diet. *Metabolism* **51**, 864–870 (2002).
66. M. Rosenbaum, K. D. Hall, J. Guo, E. Ravussin, L. S. Mayer, M. L. Reitman, S. R. Smith, B. T. Walsh, R. L. Leibel, Glucose and lipid homeostasis and inflammation in humans following an isocaloric ketogenic diet. *Obesity* **27**, 971–981 (2019).
67. E. C. Westman, W. S. Yancy, J. C. Mavropoulos, M. Marquart, J. R. McDuffie, The effect of a low-carbohydrate, ketogenic diet versus a low-glycemic index diet on glycemic control in type 2 diabetes mellitus. *Nutr. Metab.* **5**, 36 (2008).
68. J. Z. Goldenberg, A. Day, G. D. Brinkworth, J. Sato, S. Yamada, T. Jönsson, J. Beardsley, J. A. Johnson, L. Thabane, B. C. Johnston, Efficacy and safety of low and very low carbohydrate diets for type 2 diabetes remission: Systematic review and meta-analysis of published and unpublished randomized trial data. *BMJ* **372**, m4743 (2021).
69. B. B. Kahn, J. S. Flier, Obesity and insulin resistance. *J. Clin. Invest.* **106**, 473–481 (2000).
70. M. P. Czech, M. Tencerova, D. J. Pedersen, M. Aouadi, Insulin signalling mechanisms for triacylglycerol storage. *Diabetologia* **56**, 949–964 (2013).
71. B. R. Thompson, S. Lobo, D. A. Bernlohr, Fatty acid flux in adipocytes: The in's and out's of fat cell lipid trafficking. *Mol. Cell. Endocrinol.* **318**, 24–33 (2010).
72. K. N. Frayn, Adipose tissue and the insulin resistance syndrome. *Proc. Nutr. Soc.* **60**, 375–380 (2001).
73. I. Trouwborst, S. M. Bowser, G. H. Goossens, E. E. Blaak, Ectopic fat accumulation in distinct insulin resistant phenotypes; targets for personalized nutritional interventions. *Front. Nutr.* **5**, 77 (2018).
74. Q.-Y. Cai, Z.-J. Zhou, R. Luo, J. Gan, S.-P. Li, D.-Z. Mu, C.-M. Wan, Safety and tolerability of the ketogenic diet used for the treatment of refractory childhood epilepsy: A systematic review of published prospective studies. *World J. Pediatr.* **13**, 528–536 (2017).
75. A. Corsello, C. M. Trovato, E. Di Profio, S. Cardile, C. Campoy, G. Zuccotti, E. Verduci, A. Diamanti, Ketogenic diet in children and adolescents: The effects on growth and nutritional status. *Pharmacol. Res.* **191**, 106780 (2023).
76. D. K. Groesbeck, R. M. Bluml, E. H. Kossoff, Long-term use of the ketogenic diet in the treatment of epilepsy. *Dev. Med. Child Neurol.* **48**, 978–981 (2006).
77. J. Choi, T. L. Young, L. B. Chartier, Recurrent acute pancreatitis during a ketogenic diet-a case report and literature review. *Int. J. Emerg. Med.* **14**, 52 (2021).
78. A. L. Hartman, E. P. G. Vining, Clinical aspects of the ketogenic diet. *Epilepsia* **48**, 31–42 (2007).
79. C.-C. Li, C.-C. Chang, Y.-G. Cherng, C.-S. Lin, C.-C. Yeh, Y.-C. Chang, C.-J. Hu, C.-C. Shih, T.-L. Chen, C.-C. Liao, Risk and outcomes of diabetes in patients with epilepsy. *Sci. Rep.* **11**, 18888 (2021).
80. A. Gaitatzis, B. Purcell, K. Carroll, J. W. A. S. Sander, A. Majeed, Differences in the use of health services among people with and without epilepsy in the United Kingdom: Socio-economic and disease-specific determinants. *Epilepsy Res.* **50**, 233–241 (2002).
81. R. Kobau, H. Zahran, D. J. Thurman, M. M. Zack, T. R. Henry, S. C. Schachter, P. H. Price, Centers for Disease Control and Prevention (CDC), Prevention, epilepsy surveillance among adults—19 states, behavioral risk factor surveillance system, 2005. *MMWR Surveill. Summ.* **57**, 1–20 (2008).
82. D. McCorry, A. Nicolson, D. Smith, A. Marson, R. G. Feltbower, D. W. Chadwick, An association between type 1 diabetes and idiopathic generalized epilepsy. *Ann. Neurol.* **59**, 204–206 (2006).
83. M. Mastrangelo, V. Tromba, F. Silvestri, F. Costantino, Epilepsy in children with type 1 diabetes mellitus: Pathophysiological basis and clinical hallmarks. *Eur. J. Paediatr. Neurol.* **23**, 240–247 (2019).
84. N. A. Shlobin, J. W. Sander, Drivers for the comorbidity of type 2 diabetes mellitus and epilepsy: A scoping review. *Epilepsy Behav.* **106**, 107043 (2020).
85. M. I. Love, W. Huber, S. Anders, Moderated estimation of fold change and dispersion for RNA-seq data with DESeq2. *Genome Biol.* **15**, 550 (2014).
86. G. Wu, R. Haw, Functional interaction network construction and analysis for disease discovery. *Methods Mol. Biol.* **1558**, 235–253 (2017).
87. Y. Zhou, B. Zhou, L. Pache, M. Chang, A. H. Khodabakhshi, O. Tanaseichuk, C. Benner, S. K. Chanda, Metascape provides a biologist-oriented resource for the analysis of systems-level datasets. *Nat. Commun.* **10**, 1523 (2019).
88. A. Lex, N. Gehlenborg, H. Strobelt, R. Vuillemot, H. Pfister, UpSet: Visualization of intersecting sets. *IEEE Trans. Vis. Comput. Graph.* **20**, 1983–1992 (2014).
89. P. Bankhead, M. B. Loughrey, J. A. Fernández, Y. Dombrowski, D. G. McArt, P. D. Dunne, S. McQuaid, R. T. Gray, L. J. Murray, H. G. Coleman, J. A. James, M. Salto-Tellez,

P. W. Hamilton, QuPath: Open source software for digital pathology image analysis. *Sci. Rep.* **7**, 16878 (2017).
90. W. Liang, A. L. Menke, A. Driessen, G. H. Koek, J. H. Lindeman, R. Stoop, L. M. Havekes, R. Kleemann, A. M. van den Hoek, Establishment of a general NAFLD scoring system for rodent models and comparison to human liver pathology. *PLOS ONE* **9**, e115922 (2014).
91. V. I. a. P. A. Core (protocols.io, 2021); www.protocols.io/view/mouse-pancreatic-islet-isolation-bp2l6boe5gqe/v1.
92. V. I. a. P. A. Core (protocols.io, 2022); www.protocols.io/view/mouse-islet-perifusion-3-stimuli-protocol-n2bvj6yenlk5/v1.

Acknowledgments: We thank additional members of the A.C. laboratory, E. Gonzalez Alvarado, C. Ural, and N. Murahari for assisting with WL study; J. Varre and D. Ramos from W.L.H.'s laboratory for the help preparing islets and performing the surgeries; and M. Wortham for sharing the islet biology expertise. We acknowledge the Metabolic Phenotyping Core (CLAMS and Bruker Minispec NMR; Y. Li), Cell Imaging Core (Axioscan Slide Scanner; A. Classen and B. James) and the Electron Microscopy Core at the University of Utah for use of equipment and thank the staff for their assistance. Research reported in this publication also used the High Throughput Genomics Core (Illumina Nextgen Sequencing; B. Dalley) and the Bioinformatics Core (RNA sequencing analysis; C. Stubben) at Huntsman Cancer Institute at the University of Utah supported by NCI P30CA042014. Ex vivo GSIS was performed by the Islet and Pancreas Analysis (IPA) Core supported by the Vanderbilt Diabetes Research Center DK20593. **Funding:** This work was supported by funds from NIA R01AG065993 and the DRC at Washington University NIH P30DK020579 to A.C., NIDDK F32DK137475, and T32DK110966 to M.R.G. W.L.H. receives funds from DK108833, DK112826, and HL170575. K.J.E. is funded in part by Damon Runyon-Rachleff Innovation Award DR 61-20, NCI R01CA222570, and the American Cancer Society (RSG-22-014-01-CCB). **Author contributions:** Conceptualization, M.R.G., A.C., and W.L.H. Methodology: M.R.G., A.C., W.L.H., W.L., and E.T.M. Investigation: M.R.G., A.C., W.L.H., R.F.L.V., E.T.M., P.D.M., F.E.S., S.R., W.L., and K.J.E. Writing—original draft: M.R.G. Writing—review and editing: M.R.G., A.C., and W.L.H. Funding acquisition: A.C. Resources: A.C., W.L.H., K.J.E., and W.L. Supervision: W.L.H. and A.C. **Competing interests:** All authors declare that they have no competing interests. **Data and materials availability:** All data needed to evaluate the conclusions in the paper are present in the paper and/or the Supplementary Materials. Fastq files are available online. Liver RNA sequencing (GEO, GSE244492) and islet RNA sequencing (GE, GSE268020): www.ncbi.nlm.nih.gov/geo/query/acc.cgi?acc=GSE248297 and www.ncbi.nlm.nih.gov/geo/query/acc.cgi?acc=GSE268020.

Submitted 7 March 2025
Accepted 19 August 2025
Published 19 September 2025
10.1126/sciadv.adx2752